Electronic Supplementary Information

for

Ring-fused porphyrins: extension of π-conjugation significantly affects the aromaticity and optical properties of the porphyrin π-systems and Lewis acidity of the central metal ions

Yuta Saegusa,[a] Tomoya Ishizuka,[a] Keiyu Komamura,[a] Soji Shimizu,[b] Hiroaki Kotani,[a] Nagao Kobayashi,[b] and Takahiko Kojima*[a]*

[a]Department of Chemistry, Graduate School of Pure and Applied Sciences, University of Tsukuba, 1-1-1 Tennoudai, Tsukuba, Ibaraki 305-8571, Japan

[b]Department of Chemistry, Graduate School of Science, Tohoku University, Sendai 980-8578, Japan

Experimental section

Synthesis.

A general procedure[1] of Pd-catalysed ring-fusing reactions Using Pd-nanoclusters[2] with $[Pd(\eta^2\text{-}C_3H_5)Cl]_2$. A solution of TBA·OAc (TBA = tetra(*n*-butyl)ammonium, 627 mg, 2.08 mmol), allyl palladium(II) chloride dimer (3.53 mg, 9.65 μmol), and potassium carbonate (279 mg, 2.03 mmol) in 1,4-dioxane (1.0 mL) was heated at 110 ºC for 3 min. After the colour of the solution changed to black, a tetrabromo-derivative of porphyrin (50 μmol) was quickly added to the solution. After stirring for 11 h, the reaction mixture was cooled to ambient temperature. The volatiles were removed under vacuum and the residual solid was washed with water. The solid was dissolved in pyridine and the precipitate including the palladium catalyst was filtered off. The filtrate was dried *in vacuo* to give black powder and the black powder was recrystallized from the THF solution in the presence of one drop of pyridine by depositing ethanol vapour as a poor solvent. The crystals obtained was filtered and washed with THF to give a red-purple filtrate. The remaining dark red solid mainly involved the quadruply-fused derivative and the further recrystallization by vapour deposition of ethanol to the THF solution in the presence of one drop of pyridine to give pure QFP derivative.

Zinc(II) *trans*-doubly-fused porphyrinate (2-*trans*). A solution of TBA·OAc (627 mg, 2.08 mmol), palladium acetate (4.81 mg, 21 μmol), triphenylphosphine (10.5 mg, 40 μmol), Molecular Sieves 4A (70 mg), potassium carbonate (280 mg, 2.03 mmol), and **12a** (50.2 mg, 51 μmol) in 1,4-dioxane (1.0 mL) was stirred at 110 ºC for 16 h. The reaction mixture was cooled to ambient temperature, filtered, and washed with water. The red-brown powder was chromatographed on a silica gel column by using CH_2Cl_2/hexane (1:1, v/v) as an eluent to give ZnTPP (3.3 mg, 18 μmol, 10%), **1** (8.7 mg, 13 μmol, 25%), **2** (13 mg, 20 μmol, 40%), and **3** (5.0 mg, 7.4 μmol, 15%). **2** was a mixture of **2**-*cis* and **2**-*trans* and chromatographed on a GPC-HPLC by using $CHCl_3$ as an eluent. The recrystallization from THF/CH_3OH gave light red powder of **2**-*cis* (6 mg, 9.2 μmol) and dark red powder of **2**-*trans* (4 mg, 4 μmol). m.p.: >300 ºC. ^{1}H NMR (DMSO-d_6): δ 8.99 (d, J = 4.2 Hz, 2H, 12-β-H), 8.17 (d, J = 4.2 Hz, 2H, 13-β-H), 8.11 (d, J = 7.7 Hz, 2H, 29,41-Ph-H), 8.00-7.90 (m, 4H, *o*-Ph-H), 7.75-7.66 (m, 6H, *m*, *p*-Ph-H), 7.56 (s, 2H, 7,17-β-H), 7.36 (d, 2H, J = 7.7 Hz, 32,44-Ph-H), 7.02 (t, J = 7.7 Hz, 2H, 30,42-Ph-H), 6.91 (t, J = 7.7 Hz, 2H, 31,43-Ph-H). UV-vis (DMF): λ_{max} [nm] (log (ε, M^{-1} cm^{-1})) = 432 (4.58), 489 (5.08), 522 (4.69), 643 (3.97), 721 (3.73), 799 (3.71), 895 (3.75). MS (MALDI-TOF, *dithranol* matrix): m/z = 674.1 $[M]^+$ (calcd. 674.1).

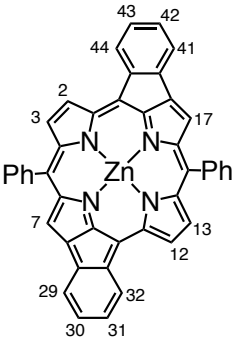

Zinc(II) 24,30,36,42-tetrakis(*tert*-butyl)-quadruply-fused porphyrinate (5). A ring-fusion reaction was performed utilizing **12b** (130.3 mg, 107 μmol) as a starting material to obtain **5**, using the aforementioned general procedure. After filtration, the precipitate obtained was chromatographed on a Bio-Beads S-X1 gel using THF as an eluent. The second fraction was collected and the solvent was removed *in vacuo*. The residual solid was recrystallized from THF/ethanol (1:3, v/v) and dried under vacuum to give **5** (69.0 mg, 77.1 μmol, 72%). m.p.: >300 ºC. ^{1}H NMR (DMSO-d_6): δ 7.89 (s,

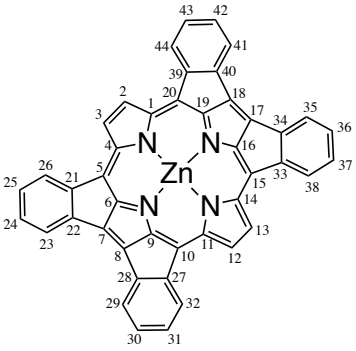

4H, 2, 3,12,13-β-H), 7.20 (d, J = 8.0 Hz, 4H, 26,32,38,44-Ph-H), 6.87 (s, 4H, 23,29,35,41-Ph-H), 6.74 (m, 4H, 25,31,37,43-Ph-H), 1.32 (s, 36H, *tert*-Bu-H). UV-vis (DMF): λ_{max} [nm] (log (ε, M^{-1} cm^{-1})) = 334 (4.49), 408 (4.52), 489 (4.34), 616 (4.81), 778 (3.72), 934 (3.38), 1060 (3.26). MS (MALDI-TOF, *dithranol matrix*): *m/z* = 892.4 $[M]^+$ (calcd. 892.4). Anal. Calcd for $C_{60}H_{52}N_4Zn \cdot H_2O \cdot$pyridine: C, 78.73; H, 6.00; N, 7.06. Found: C, 78.66; H, 5.82; N, 6.98.

Zinc(II) 24,30,36,42-tetramethoxy-quadruply-fused porphyrinate (6). A ring-fusion reaction using the above-mentioned general procedure was performed utilizing **12c** (59.7 mg, 53.6 μmol) as a starting material to obtain **6**. After filtration, the precipitate obtained was chromatographed on a Bio-Beads S-X1 gel using THF as an eluent. The second fraction was collected and the solvent was removed *in vacuo*. The residual solid was recrystallized from THF/ethanol (1:3, v/v) and dried under vacuum to give **6** (27.8 mg, 35.3 μmol, 65%). m.p.: >300 ºC. ^{1}H NMR (DMSO-d_6): δ 8.09 (s, 4H, 2, 3,12,13-β-H), 7.41 (d, J = 7.4 Hz, 4H, 26,32,38,44-Ph-H), 6.70 (s, 4H, 23,29,35,41-Ph-H), 6.37 (m, 4H, 25,31,37,43-Ph-H), 3.81 (s, 12H, methoxy-H). UV-vis (DMF): λ_{max} [nm] (log (ε, M^{-1} cm^{-1})) = 347 (4.52), 399 (4.34), 467 (4.59), 637 (4.71), 803 (3.66), 913 (3.26), 1026 (3.11), 1200 (2.99). MS (MALDI-TOF, *dithranol matrix*): *m/z* = 788.5 $[M]^+$ (calcd. 788.1). Anal. Calcd for $C_{48}H_{28}N_4O_4Zn \cdot 0.5H_2O \cdot 0.25THF \cdot 0.5CH_2Cl_2$: C, 69.16; H, 3.75; N, 6.52. Found: C, 68.99; H, 3.79; N, 6.29.

Zinc(II) 24,30,36,42-tetra(methoxycarbonyl)-quadruply-fused porphyrinate (7). A ring-fusion reaction using the general procedure mentioned above was performed utilizing **12d** (61.5 mg, 50.2 μmol) as a starting material to obtain **7**. After filtration, the collected solid was recrystallized from pyridine/ethanol (1:3, v/v) and dried under vacuum to give pure **7** (10.4 mg, 11.0 μmol, 22%). m.p.: >300 ºC. ^{1}H NMR (DMSO-d_6): δ 8.28 (s, 4H, 2, 3,12,13-β-H), 7.74 (m, 4H, 26,32,38,44-Ph-H), 7.52-7.42 (m, 8H, 23,25,29,31,35,37,41,43-Ph-H). UV-vis (DMF): λ_{max} [nm] (log (ε, M^{-1} cm^{-1})) = 420 (4.40), 491 (4.23), 604 (4.50), 721 (3.91), 815 (3.61), 1028 (3.13). MS (MALDI-TOF, *dithranol matrix*): *m/z* = 1161.6 [M + dithranol – 2H + K]$^+$ (calcd. 1162.1). Anal. Calcd for $C_{52}H_{28}N_4O_8Zn \cdot 3H_2O$: C, 65.31; H, 3.58; N, 5.86. Found: C, 65.11; H, 3.68; N, 5.60.

Zinc(II) 24,30,36,42-tetrakis(trifluoromethyl)-quadruply-fused porphyrinate (8). A ring-fusion reaction using the aforementioned general procedure was performed utilizing **12e** (62.6 mg, 49.3 μmol) as a starting material to obtain **8**. After filtration, the remaining dark red solid mainly including **8** was recrystallized by vapour deposition of ethanol as a poor solvent to the THF solution in the presence of one drop of pyridine to give pure **8** (10.2 mg, 10.8 μmol, 22%). m.p.: >300 ºC. ^{1}H NMR (DMSO-d_6): δ 8.17 (s, 4H, 2,3,12,13-β-H), 7.68 (d, J = 7.4 Hz, 4H, 26,32,38,44-Ph-H), 7.25-7.15 (m, 8H, 23,25,29,31,35,37,41,43-Ph-H). UV-vis (DMF): λ_{max} [nm] (log (ε, M^{-1} cm^{-1})) = 320 (4.64), 403 (4.66), 497 (4.43), 598 (4.95), 793 (4.66), 929 (3.57), 1104 (3.18). MS (MALDI-TOF, *dithranol matrix*): *m/z* = 940.3 $[M]^+$ (calcd. 940.1). Anal. Calcd for $C_{48}H_{16}N_4F_{12}Zn \cdot H_2O \cdot C_2H_5OH$: C, 59.69; H, 2.40; N, 5.57. Found: C, 59.82; H, 2.46; N, 5.55.

24,30,36,42-tetramesityl-quadruply-fused porphyrin (9). A ring-fusion reaction according to the general procedure mentioned above was performed utilizing **12f** (73 mg, 50 μmol) as a starting material to obtain **9**. After filtration, the precipitate obtained was chromatographed on a Bio-Beads S-X1 gel using THF as an eluent. The second moving fraction was collected and the solvent was removed *in vacuo*. The residual solid was recrystallized from THF/ethanol (1:3, v/v) and

Scheme S1.

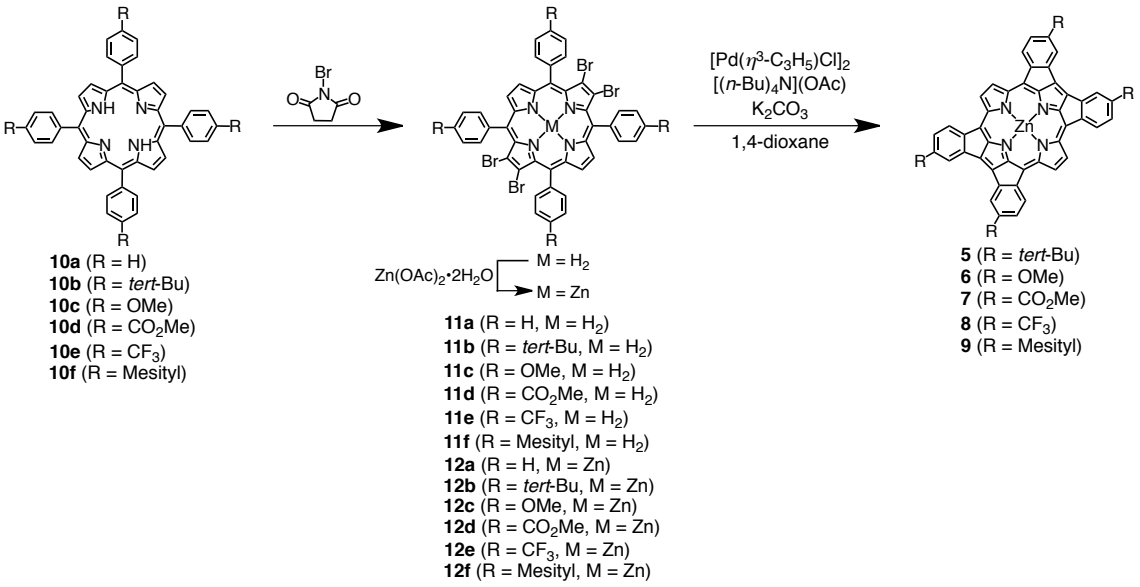

10a (R = H)
10b (R = *tert*-Bu)
10c (R = OMe)
10d (R = CO_2Me)
10e (R = CF_3)
10f (R = Mesityl)

11a (R = H, M = H_2)
11b (R = *tert*-Bu, M = H_2)
11c (R = OMe, M = H_2)
11d (R = CO_2Me, M = H_2)
11e (R = CF_3, M = H_2)
11f (R = Mesityl, M = H_2)
12a (R = H, M = Zn)
12b (R = *tert*-Bu, M = Zn)
12c (R = OMe, M = Zn)
12d (R = CO_2Me, M = Zn)
12e (R = CF_3, M = Zn)
12f (R = Mesityl, M = Zn)

5 (R = *tert*-Bu)
6 (R = OMe)
7 (R = CO_2Me)
8 (R = CF_3)
9 (R = Mesityl)

dried under vacuum to give pure **9** (42 mg, 37 μmol, 74%). m.p.: >300 ºC. ^{1}H NMR (DMSO-d_6): δ 8.35 (s, 4H, 2, 3,12,13-β-H), 7.71 (d, J = 7.6 Hz, 4H, 26,32,38,44-Ph-H), 6.95 (s, 4H, 23,29,35,41-Ph-H), 6.90 (s, 8H, *m*-mesityl-H), 6.54 (d, J = 7.6 Hz, 4H, 25,31,37,43-Ph-H), 2.23 (s, 12H, mesityl-*p*-CH_3), 2.11 (s, 24H, mesityl-*o*-CH_3). UV-vis (THF): λ_{max} [nm] (log (ε, M^{-1} cm^{-1})) = 320 (4.61), 412 (4.65), 437 (4.62), 598 (4.98), 616 (4.97), 775 (3.80), 918 (3.38), 1046 (3.15). MS (MALDI-TOF, *dithranol matrix*): *m/z* = 1140.4 $[M]^+$ (calcd. 1140.8). Anal. Calcd for $C_{80}H_{60}N_4Zn{\cdot}5H_2O{\cdot}CH_2Cl_2$: C, 73.83; H, 5.51; N, 4.25. Found: C, 73.64; H, 5.70; N, 3.98.

5,10,15,20-Tetraphenylporphyrin (10a). This compound was synthesized according to the literature procedure[3] to yield a purple solid of **10a** (787 mg, 1.3 mmol, 19%). ^{1}H NMR ($CDCl_3$): δ 8.84 (s, 8H, β-H), 8.22 (dd, J = 8.0, 1.6 Hz, 4H, *o*-phenyl-H), 7.72-7.78 (m, 12H, *m*, *p*-phenyl-H), –2.77 (br s, 2H, inner N*H*). UV-vis ($CHCl_3$): λ_{max} [nm] = 647, 591, 550, 512, 418. Fluorescence (λ_{ex} = 418 nm, $CHCl_3$): λ_{max} [nm] = 714, 649. MS (MALDI-TOF, dithranol matrix): *m/z* = 613.9 $[M]^+$ (calcd. 614.3).

5,10,15,20-Tetrakis(4-*tert*-butylphenyl)porphyrin (10b).[4] A condensation of pyrrole (2.79 mL, 40.2 mmol) and 4-*tert*-butylbenzaldehyde (6.72 mL, 40.1 mmol) was performed with a similar procedure of **10a** to obtain **10b** (2.03 g, 2.4 mmol, 24%). ^{1}H NMR ($CDCl_3$): δ 8.97 (s, 8H, β-H), 8.15 (d, J = 8.3 Hz, 4H, *o*-phenyl-H), 7.76 (d, J = 8.3 Hz, 4H, *m*-phenyl-H), –2.77 (br s, 2H, inner N*H*). UV-vis ($CHCl_3$): λ_{max} [nm] = 648, 592, 554, 518, 421. MS (MALDI-TOF, dithranol matrix): *m/z* = 841.1 $[M]^+$ (calcd. 841.5).

5,10,15,20-Tetrakis(4-methoxyphenyl)porphyrin (10c).[5,6] A condensation of pyrrole (2.78 mL, 40.2 mmol) and 4-methoxyphenylbenzaldehyde (4.88 mL, 40.2 mmol) was performed with a similar procedure of **10a** to obtain **10c** (1.38 g, 1.9 mmol, 19%). ^{1}H NMR ($CDCl_3$): δ 8.86 (s, 8H, β-H), 8.12 (d, J = 8.6 Hz, 4H, *o*-phenyl-H), 7.29 (d, J = 8.6 Hz, 8H, *m*-phenyl-H), 4.10 (s, 12H, metoxy-H), –2.74 (br s, 2H, inner N*H*). UV-vis ($CHCl_3$): λ_{max} [nm] = 651, 594, 556, 520, 422. MS (MALDI-TOF, dithranol matrix): *m/z* = 798.3 $[M]^+$ (calcd. 798.2).

5,10,15,20-Tetrakis(4-methoxycarbonylphenyl)porphyrin (10d).[6] A condensation of pyrrole (2.79 g, 40.2 mmol) and 4-methoxycarbonylbenzaldehyde (6.62 g, 40.2 mmol) was performed with a similar procedure of **10a** to obtain **10d** (2.35 g, 2.8 mmol, 28%). ^{1}H NMR ($CDCl_3$): δ 8.82 (s, 8H, β-H), 8.45 (d, J = 6.5 Hz, 8H, *o*-phenyl-H), 8.30 (d, J = 6.5 Hz, 8H, *m*-phenyl-H), 4.12 (s, 12H, CO_2CH_3), –2.81 (br s, 2H, inner N*H*). UV-vis ($CHCl_3$): λ_{max} [nm] = 648, 589, 550, 517, 421. MS (MALDI-TOF, dithranol matrix): m/z = 846.1 $[M]^+$ (calcd. 846.3).

5,10,15,20-Tetrakis(4-trifluoromethylphenyl)porphyrin (10e).[7] A condensation of pyrrole (2.09 mL, 30.2 mmol) and 4-trifluoromethylbenzaldehyde (4.05 mL, 30.2 mmol) was performed with a similar procedure of **10a** to obtain **10e** (1.06 g, 1.20 mmol, 16%). ^{1}H NMR ($CDCl_3$): δ 8.81 (s, 8H, β-H), 8.34 (d, J = 8.0 Hz, 4H, *o*-phenyl-H), 8.05 (d, J = 8.0 Hz, 8H, *m*-phenyl-H), –2.84 (br s, 2H, inner N*H*). UV-vis ($CHCl_3$): λ_{max} [nm] = 645, 589, 548, 513, 418. MS (MALDI-TOF, dithranol matrix): m/z = 885.7 $[M]^+$ (calcd. 885.2).

Scheme S2.

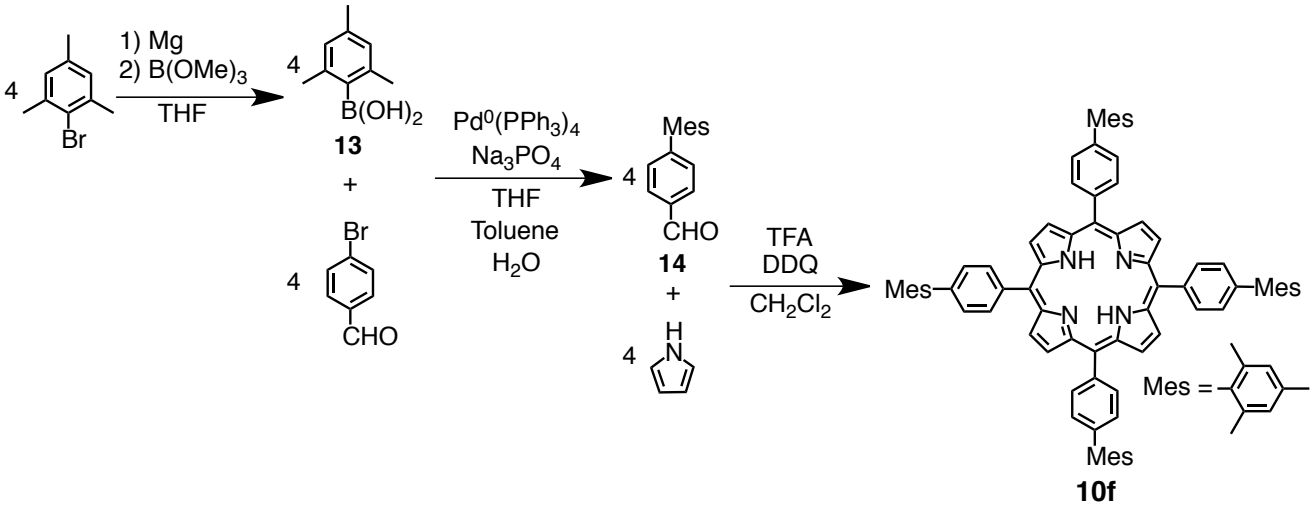

5,10,15,20-Tetrakis(4-mesitylphenyl)porphyrin (10f).[8] To the solution of **14** (3.15 g, 15 mmol) in CH_2Cl_2 (1.5 L) was added pyrrole (1.04 mL, 15 mmol), and subsequently, trifluoroacetic acid (2.24 mL, 30 mmol), and the reaction mixture was stirred at room temperature for 3 h. To the resultant solution, was added DDQ (= 2,3-dichloro-5,6-dicyanobenzoquinone) (1.71 g, 7.5 mmol) and the reaction mixture was further stirred at room temperature for 1 h. The reaction mixture was poured onto an alumina pad and eluted with CH_2Cl_2 until the eluting solution became pale brown. The solvent was removed under vacuum to give a purple solid. The resulting purple powder was chromatographed on a silica gel column by using CH_2Cl_2/hexane (3:4, v/v) as an eluent. The red purple fraction was collected and the solvent was removed *in vacuo*. The residual solid was recrystallized from CH_2Cl_2/CH_3OH (1:3, v/v) and dried under vacuum to yield **10f** (843 mg, 0.77 mmol, 21%). ^{1}H NMR ($CDCl_3$): δ 8.99 (s, 8H, β-H), 8.30 (dd, J = 6.3, 1.9 Hz, 4H, *o*-phenyl-H), 7.54 (dd, J = 6.3, 1.9 Hz, 8H, *m*, *p*-phenyl-H), 7.12 (s, 8H, *m*-mesityl-H), 2.44 (s, 12H, mesityl-*p*-CH_3), 2.36 (s, 24H, mesityl-*o*-CH_3), –2.65 (br s, 2H, inner

N*H*). UV-vis ($CHCl_3$): λ_{max} [nm] = 648, 593, 553, 518, 421. MS (MALDI-TOF, dithranol matrix): *m/z* = 1150.85 $[M]^+$ (calcd. 1150.84).

2,3,12,13-Tetrabromo-5,10,15,20-tetraphenylporphyrin (11a).[9,10] To a solution of **10a** (303.2 mg, 0.49 mmol) in $CHCl_3$ (60 mL) was added recrystallized *N*-bromosuccinimide (NBS) (532 mg, 2.99 mmol) and the reaction mixture was refluxed for 4 h. After cooling to room temperature, the reaction mixture was washed with water to remove any soluble succinimide impurities. The brown-coloured solid was chromatographed on a silica gel column using $CHCl_3$/hexane (1:3, v/v) as an eluent. The first moving fraction was collected and the solvent was removed *in vacuo*. The residual solid was recrystallized from CH_2Cl_2/CH_3OH (1:3, v/v) and dried under vacuum to yield **11a** (280 mg, 0.30 mmol, 61%). ^{1}H NMR ($CDCl_3$): δ 8.70 (s, 4H, β-H), 8.17 (d, J = 8.0 Hz, 8H, *o*-phenyl-H), 7.75-7.81 (m, 12H, *m*, *p*-phenyl-H), –2.82 (br s, 2H, inner N*H*). UV-vis ($CHCl_3$): λ_{max} [nm] = 684, 536, 438. MS (MALDI-TOF, dithranol matrix): *m/z* = 927.1 $[M + H]^+$ (calcd. 926.9).

2,3,12,13-Tetrabromo-5,10,15,20-tetrakis(4-*tert*-butylphenyl)porphyrin (11b).[11] A bromination reaction was performed utilizing **10b** (1.00 g, 1.19 mmol) as a starting material and NBS (1.74 g, 9.76 mmol) to obtain **11b** (758 mg, 0.65 mmol, 55%) with a method as described in the synthesis of **11a**. ^{1}H NMR ($CDCl_3$): δ 8.84 (s, 8H, β-H), 8.22 (dd, J = 8.0, 1.6 Hz, 4H, *o*-phenyl-H), 7.72-7.78 (m, 12H, *m*, *p*-phenyl-H), –2.77 (br s, 2H, inner N*H*). UV-vis ($CHCl_3$): λ_{max} [nm] = 699, 543, 444. MS (MALDI-TOF, dithranol matrix): *m/z* = 1154.7 $[M + 4H]^+$ (calcd. 1154.2).

2,3,12,13-Tetrabromo-5,10,15,20-tetrakis(4-methoxyphenyl)porphyrin (11c).[11] A bromination reaction with a similar procedure of **11a** was performed utilizing **10c** (507 mg, 0.68 mmol) and NBS (564 mg, 3.26 μmol) as starting materials to obtain **11c** (544 mg, 0.52 mmol, 76%). ^{1}H NMR ($CDCl_3$): δ 8.69 (s, 4H, β-H), 8.10 (d, J = 8.6 Hz, 4H, *o*-phenyl-H), 732 (d, J = 8.6 Hz, 8H, *m*-phenyl-H), 4.10 (s, 12H, methoxy-H), –2.71 (br s, 2H, inner N*H*). UV-vis ($CHCl_3$): λ_{max} [nm] = 699, 590, 543, 446. MS (MALDI-TOF, dithranol matrix): *m/z* = 1051.2 $[M + H]^+$ (calcd. 1050.9).

2,3,12,13-Tetrabromo-5,10,15,20-tetrakis(4-methoxycarbonylphenyl)porphyrin (11d).[11] A bromination reaction with a similar procedure of **11a** was performed utilizing **10d** (600 mg, 0.71 mmol) as a starting material in 1,2-dichloroethane (150 mL) to obtain **11d**. After washing with H_2O and removal of the solvent, the reaction mixture was chromatographed on a silica gel column by using CH_2Cl_2/CH_3OH/Et_3N (100:3:0.5, v/v/v) as an eluent. The second moving fraction was collected and the solvent was removed *in vacuo*. The residual solid was recrystallized from CH_2Cl_2/CH_3OH (1:3, v/v) and the crystalline solid obtained was dried under vacuum to yield **11d** (389 mg, 0.33 mmol, 47%). ^{1}H NMR ($CDCl_3$): δ 8.65 (s, 4H, β-H), 8.46 (d, J = 8.0 Hz, 8H, *o*-phenyl-H), 8.25 (d, J = 8.0 Hz, 8H, *m*-phenyl-H), 4.11 (s, 12H, CO_2CH_3), –2.85 (br s, 2H, inner N*H*). UV-vis ($CHCl_3$): λ_{max} [nm] = 681, 615, 535, 439. MS (MALDI-TOF, dithranol matrix): *m/z* = 1162.9 $[M]^+$ (calcd. 1162.9).

2,3,12,13-Tetrabromo-5,10,15,20-tetrakis(4-mesitylphenyl)porphyrin (11f). A bromination reaction with a similar procedure of **11d** was performed utilizing **10f** (426 mg, 0.39 mmol) as a starting material to obtain **11f** (374 mg, 0.27 mmol, 69%). ^{1}H NMR ($CDCl_3$): δ 8.87 (s, 4H, β-H), 8.26 (d, J = 8.0 Hz, 4H, *o*-phenyl-H), 7.57 (d, J = 8.0 Hz, 8H, *m*-phenyl-H), 7.11 (s, 8H, *m*-mesityl-H), 2.43 (s, 12H, mesityl-*p*-CH_3), 2.33 (s, 24H, mesityl-*o*-CH_3), –2.70 (br s, 2H, inner N*H*). UV-vis ($CHCl_3$): λ_{max} [nm]= 690, 539, 442. MS (MALDI-TOF, dithranol matrix): *m/z* = 1403.2 $[M + H]^+$ (calcd. 1403.2).

Zinc(II) 2,3,12,13-tetrabromo-5,10,15,20-tetraphenylporphyrinate (12a).[11,12] To a solution of **11a** (260 mg, 0.262 mmol) in $CHCl_3$ (50 mL), was added a suspension of $Zn(OAc)_2 \cdot 2H_2O$ (311 mg, 1.42 mmol) in CH_3OH (20 mL) and the reaction mixture was refluxed for 5 h. The reaction mixture was poured into water and the organic phase was separated and then dried over Na_2SO_4. After removing the solvent, the resulting red purple powder was chromatographed on a silica gel column by using $CHCl_3$/hexane (3:1, v/v) as an eluent. The second moving fraction was collected and the solvent was removed *in vacuo*. The residual solid was recrystallized from CH_2Cl_2/hexane (1:3, v/v) and the crystalline solid obtained was dried under vacuum to yield **12a** (217 mg, 0.22 mmol, 83%). ^{1}H NMR ($CDCl_3$): δ 8.65 (s, 4H, β-H), 8.02 (d, J = 8.0 Hz, 8H, *o*-phenyl-H), 7.66-7.77 (m, 12H, *m*, *p*-phenyl-H). UV-vis ($CHCl_3$): λ_{max} [nm] = 597, 557, 431. MS (MALDI-TOF, dithranol matrix): *m/z* = 988.3 $[M + H]^+$ (calcd. 988.8).

Zinc(II) 2,3,12,13-tetrabromo-5,10,15,20-tetrakis(4-*tert*-butylphenyl)porphyrinate (12b).[13] Metalation of **11b** with a similar procedure of **12a** was performed utilizing **11b** (385 mg, 0.33 mmol) and $Zn(OAc)_2 \cdot 2H_2O$ (362 mg, 1.65 mmol) as starting materials to obtain **12b** (310 mg, 0.25 mmol, 76%). ^{1}H NMR ($CDCl_3$): δ 8.65 (s, 4H, β-H), 8.02 (d, J = 8.0 Hz, 8H, *o*-phenyl-H), 7.66-7.77 (m, 12H, *m*, *p*-phenyl-H). UV-vis ($CHCl_3$): λ_{max} [nm] = 611, 598, 437. MS (MALDI-TOF, dithranol matrix): *m/z* = 1221.7 $[M + 3H]^+$ (calcd. 1221.2).

Zinc(II) 2,3,12,13-tetrabromo-5,10,15,20-tetrakis(4-methoxyphenyl)porphyrinate (12c). Metalation of **11c** with a similar procedure of **12a** was performed utilizing **11c** (396 mg, 0.38 mmol) and $Zn(OAc)_2 \cdot 2H_2O$ (417 mg, 1.9 mmol) as starting materials to obtain **12c** (378 mg, 0.34 mmol, 89%). ^{1}H NMR ($CDCl_3$): δ 8.57 (s, 4H, β-H), 7.92 (d, J = 8.2 Hz, 8H, *o*-phenyl-H), 7.23 (d, J = 8.2 Hz, 8H, *m*-phenyl-H), 4.07 (s, 12H, O*CH*$_3$). UV-vis ($CHCl_3$): λ_{max} [nm] = 613, 568, 439. MS (MALDI-TOF, dithranol matrix): *m/z* = 1114.9 $[M + H]^+$ (calcd. 1114.8).

Zinc(II) 2,3,12,13-tetrabromo-5,10,15,20-tetrakis(4-methoxycarbonylphenyl)porphyrinate (12d).[13] Metalation of **11d** with a similar procedure of **12a** was performed utilizing **11d** (352 mg, 0.30 mmol) and $Zn(OAc)_2 \cdot 2H_2O$ (329 mg, 1.5 mmol) as starting materials to obtain **12d** (217 mg, 0.18 mmol, 68%). ^{1}H NMR ($CDCl_3$): δ 8.57 (s, 4H, β-H), 8.36 (d, J = 7.9 Hz, 8H, *o*-phenyl-H), 8.11 (d, J = 7.9 Hz, 8H, *m*-phenyl-H), 4.08 (s, 12H, CO_2CH_3). UV-vis ($CHCl_3$): λ_{max} [nm] = 681, 567, 436. MS (MALDI-TOF, dithranol matrix): *m/z* = 1227.6 $[M + H]^+$ (calcd. 1226.8).

Zinc(II) 2,3,12,13-tetrabromo-5,10,15,20-tetrakis(4-trifluoromethylphenyl)porphyrinate (12e). To a solution of **10e** (203 mg, 0.23 mmol) in 1,2-dichloroethanne (50 mL) was added recrystallized NBS (234 mg, 1.35 mmol) and the reaction mixture was refluxed for 24 h. The solvent was removed *in vacuo*, and the residual solid was washed with H_2O and dried under vacuum to obtain crude **11e**. To the solution of crude **11e** (273 mg, 0.23 mmol) in $CHCl_3$ (45 mL) was added a suspension of $Zn(OAc)_2 \cdot 2H_2O$ (359 mg, 1.1 mmol) in CH_3OH (16 mL) and the reaction mixture was refluxed for 3 h. The reaction mixture was poured into water and the organic phase was separated and then dried over Na_2SO_4. After removing the solvent, the resulting red purple powder was chromatographed on a silica gel column by using $CHCl_3$/hexane (2:1, v/v) as an eluent. The second moving fraction was collected and the solvent was removed *in vacuo*. The residual solid was recrystallized from CH_2Cl_2/hexane (1:3, v/v) and dried under vacuum to yield **12e** (85 mg, 67 μmol, 30% (2 step)). ^{1}H NMR ($CDCl_3$): δ 8.65 (s, 4H, β-H), 8.02 (d, J = 8.0 Hz, 8H, *o*-phenyl-H), 7.66-7.77 (m, 12H, *m*, *p*-phenyl-H). UV-vis

($CHCl_3$): λ_{max} [nm] = 605, 565, 434. MS (MALDI-TOF, dithranol matrix, negative mode): *m/z* = 1226.8 $[M + H]^-$ (calcd. 1226.7).

Zinc(II) 2,3,12,13-tetrabromo-5,10,15,20-tetrakis(4-mesitylphenyl)porphyrinate (12f). Metalation of **11f** with a similar procedure of **12a** was performed utilizing **11f** (301 mg, 0.21 mmol) and $Zn(OAc)_2 \cdot 2H_2O$ (230 mg, 1.1 mmol) as starting materials to obtain **12f** (297 mg, 0.20 mmol, 95%). ^{1}H NMR ($CDCl_3$): δ 8.95 (s, 4H, β-H), 8.13 (d, J = 7.8 Hz, 4H, *o*-phenyl-H), 7.51 (d, J = 7.8 Hz, 8H, *m*-phenyl-H), 7.11 (s, 8H, *m*-mesityl-H), 2.43 (s, 12H, mesityl-*p*-CH_3), 2.35 (s, 24H, mesityl-*o*-CH_3). UV-vis ($CHCl_3$): λ_{max} [nm] = 610, 568, 437. MS (MALDI-TOF, dithranol matrix): *m/z* = 1466.6 $[M + 2H]^+$ (calcd. 1466.2).

2,4,6-Trimethylphenylboronic acid (13). This compound was synthesized according to the literature procedure.[14] ^{1}H NMR (DMSO-d_6): δ 8.05 (s, 2H, OH-H), 6.73 (s, 2H, *m*-mesityl-H), 2.22 (s, 6H, mesityl-*o*-CH_3), 2.19 (s, 3H, mesityl-*p*-CH_3).

Mesityl-benzaldehyde (14). This compound was synthesized according to a similar procedure.[15] Into a 500 mL three-necked flask equipped with a teflon magnetic stirring bar were charged **7** (10.1 g, 61.6 mmol), 4-bromobanzaldehyde (6.75 g, 36.5 mmol), Na_3PO_4 (25 g, 153 mmol) and $Pd(PPh_3)_4$ (624 mg, 0.546 mmol). Then, THF (100 mL), toluene (100 mL) and H_2O (32 mL) were added and the reaction mixture was refluxed for 8 d. The solvent was removed to give a white solid and the residual solid was dissolved in EtOAc. The reaction mixture was washed with water and dried over Na_2SO_4, and the solvent was evaporated. The white solid obtained was chromatographed on a silica gel column using EtOAc/hexane (1:6, v/v) as an eluent. The second moving fraction was collected and the solvent was removed *in vacuo* to yield **8** (8.04 g, 35.8 mmol, 98%). ^{1}H NMR ($CDCl_3$): δ 10.07 (s, 1H, C*H*O), 7.95 (d, J = 6.6 Hz, 2H, *o*-phenyl-H), 7.33 (d, J = 6.6 Hz, 2H, *m*-phenyl-H), 6.96 (s, 2H, mesityl-*m*-H), 2.34 (s, 3H, mesityl-*p*-CH_3), 1.99 (s, 6H, mesityl-*o*-CH_3).

Estimation of an association constant between a Zn^{II}-porphyrin derivative and a pyridine derivative. A solution of a Zn^{II}-porphyrin derivative was titrated with that of a pyridine derivative in CH_2Cl_2 at 298 K and the absorbance change at an appropriate wavelength was fitted with eq S1 (Figs. S13 and S14).

$$\mathrm{Abs} = \varepsilon_p[P]_0 L + (\varepsilon_{PyP}/(2 \times K)) \times (1 + K \times [py] + K \times [P]_0) - ((1 + K \times [py] + K \times [P]_0)^2 - 4 \times K^2 \times [py] \times [P]_0)^{1/2} \quad \text{(S1)}$$

Here, ε_p, [P], [py], ε_{PyP}, and K, refer to the absorption coefficient of the porphyrin derivative at a certain wavelength, the concentration of the porphyrin derivative, the concentration of the pyridine derivative, the absorption coefficient of the associated complex between the porphyrin derivative and the pyridine derivative at the corresponding wavelength, and the binding constant, respectively.

X-ray diffraction analysis. The single crystals were mounted on mounting loops. All diffraction data were collected by using a Bruker APEXII diffractometer at –153 °C (120 K) equipped with graphite-monochromated Mo Kα (λ = 0.71073

Å) by the ω-2θ scan. The structures were solved by direct methods by using SIR97 and SHELX-2013.[16] Crystallographic data for these compounds are summarized in Table S4. CCDC-1050826 (**5**-py), -1050827 (**5**-dox) and -1050828 (**8**-py), contain the supplementary crystallographic data. Recrystallization of the *t*-Bu derivative **5** from the solution in chlorobenzene in the presence of 1 drop of py by slow concentration afforded single crystals of **5**-py. On the other hand, recrystallization of **5** from the 1,4-dioxane solution by deposition of 2-propanol vapour as a poor solvent gave single crystals of **5**-dox. One molecule of **5**-py and two co-crystallized chlorobenzene molecules were involved in the asymmetric unit, whereas the asymmetric unit of the crystal of **5**-dox contained one molecule of **5**-dox and two co-crystallized dox molecules and one 2-propanol molecule. One of the two co-crystallized dox molecules in the crystal of **5**-dox was severely disordered and deleted by using the SQUEEZE program.[17] A single crystal of **8**-py was obtained by recrystallization from the pyridine solution with a vapour deposition method using MeCN as a poor solvent. Two independent molecules of **8**-py and one MeCN molecule as a co-crystallized solvent molecule were found in the asymmetric unit. The co-crystallized MeCN molecule was highly disordered and treated with the SQUEEZE program to be deleted.[17] The crystallographic parameters are summarized in Table S4.

Computational method. The structures of porphyrin derivatives were optimized by using the B3LYP functional.[18] The 6-31G(d) basis set[19,20] was used for all atoms. The program used was Gaussian 09.[21] Time-dependent density functional theory (TD-DFT)[22] has been used to calculate the excited-state energies.

Reference and Notes

(1) T. Ishizuka, Y. Saegusa, Y. Shiota, K. Ohtake, K. Yoshizawa and T. Kojima, *Chem. Commun.*, 2013, **49**, 5939.

(2) S. Higashibayashi and H. Sakurai, *Chem. Lett.*, 2007, **36**, 18.

(3) A. D. Adler, F. R. Longo, J. D. Finarelli, J. Goldmacher, J. Assour and L. Korsakoff, *J. Org. Chem.*, 1967, **32**, 476.

(4) J. Arnold, D. Y. Dawson and C. C. Hoffman, *J. Am. Chem. Soc.*, 1993, **115**, 2707.

(5) M. O'Rourke and C. Curran, *J. Am. Chem. Soc.*, 1970, **92**, 1501.

(6) K. M. Kadish and M. M. Morrison, *J. Am. Chem. Soc.*, 1976, **98**, 3326.

(7) S. S. Eaton and G. R. Eaton, *J. Am. Chem. Soc.*, 1975, **97**, 3660.

(8) J. S. Lindsey and R. W. Wagner, *J. Org. Chem.*, 1989, **54**, 828.

(9) M. J. Crossley, P. L. Burn, S. S. Chew, F. B. Cuttance and I. A. Newsom, *J. Chem. Soc., Chem. Commun.*, 1991, 1564.

(10) P. K. Kumar, P. Bhyrappa and B. Varghese, *Tetrahedron Lett.* **2003**, *44*, 4849.

(11) P. Bhyrappa, V. Velkannan, K. Karunanithi, B. Varghese and Harikrishna, *Bull. Chem. Soc. Jpn.*, 2008, **81**, 995.

(12) Y. Terazono, B. O. Patrick and D. H. Dolphin, *Inorg. Chem.*, 2002, **41**, 6703.

(13) P. Bhyrappa and V. Velkannan, *J. Porphyrins Phthalocyanines*, 2011, **15**, 883.

(14) T. Leermann, F. R. Leroux and F. Colobert, *Org Lett.*, 2011, **13**, 4479.

(15) Y. Nakayama, Y. Baba, H. Yasuda, K. Kawakita and N. Ueyama, *Macromolecules*, 2003, **36**, 7953.

(16) Sheldrick, G. M. SIR97 and SHELX97, Programs for Crystal Structure Refinement, University of Göttingen, Göttingen (Germany), 1997.

(17) P. V. D. Sluis and A. L. Spek, *Acta Crystallogr.*, 1990, **A46**, 194.

(18) (a) A. D. Becke, *Phys. Rev. A*, 1988, **38**, 3098; (b) C. Lee, W. Yang and R. G. Parr, *Phys. Rev. B*, 1988, **37**, 785; (c) A. D. Becke, *J. Chem. Phys.*, 1993, **98**, 5648.

(19) M. M. Francl, W. J. Petro, W. J. Hehre, J. S. Binkley, M. S. Gordon, D. J. DeFrees and J. A. Pople, *J. Chem. Phys.*, 1982, **77**, 3654.

(20) V. Rassolov, J. A. Pople, M. Ratner and T. L. Windus, *J. Chem. Phys.*, 1998, **109**, 1223.

(21) Gaussian 09 (Revision D.01), M. J. Frisch, G. W. Trucks, H. B. Schlegel, G. E. Scuseria, M. A. Robb, J. R. Cheeseman, G. Scalmani, V. Barone, B. Mennucci, G. A. Petersson, H. Nakatsuji, M. Caricato, X. Li, H. P. Hratchian, A. F. Izmaylov, J. Bloino, G. Zheng, J. L. Sonnenberg, M. Hada, M. Ehara, K. Toyota, R. Fukuda, J. Hasegawa, M. Ishida, T. Nakajima, Y. Honda, O. Kitao, H. Nakai, T. Vreven, J. A. Montgomery, Jr., J. E. Peralta, F. Ogliaro, M. Bearpark, J. J. Heyd, E. Brothers, K. N. Kudin, V. N. Staroverov, R. Kobayashi, J. Normand, K. Raghavachari, A. Rendell, J. C. Burant, S. S. Iyengar, J. Tomasi, M. Cossi, N. Rega, M. J. Millam, M. Klene, J. E. Knox, J. B. Cross, V. Bakken, C. Adamo, J. Jaramillo, R. Gomperts, R. E. Stratmann, O. Yazyev, A. J. Austin, R. Cammi, C. Pomelli, J. W. Ochterski, R. L. Martin, K. Morokuma, V. G. Zakrzewski, G. A. Voth, P. Salvador, J. J. Dannenberg, S. Dapprich, A. D. Daniels, Ö. Farkas, J. B. Foresman, J. V. Ortiz, J. Cioslowski and D. J. Fox, Gaussian, Inc., Wallingford CT, 2009.

(22) (a) E. K. U. Gross, J. F. Dobson and M. Petersilka, *In Density Functional Theory*; R. F. Nalewajski, Ed.; Springer: Heidelberg, 1996. (b) M. E. Casida, *In Recent Advances in Density Functional Methods*; D. P. Chong, Ed.; World Scientific: Singapore, 1995; Vol. 1, pp 155−193.

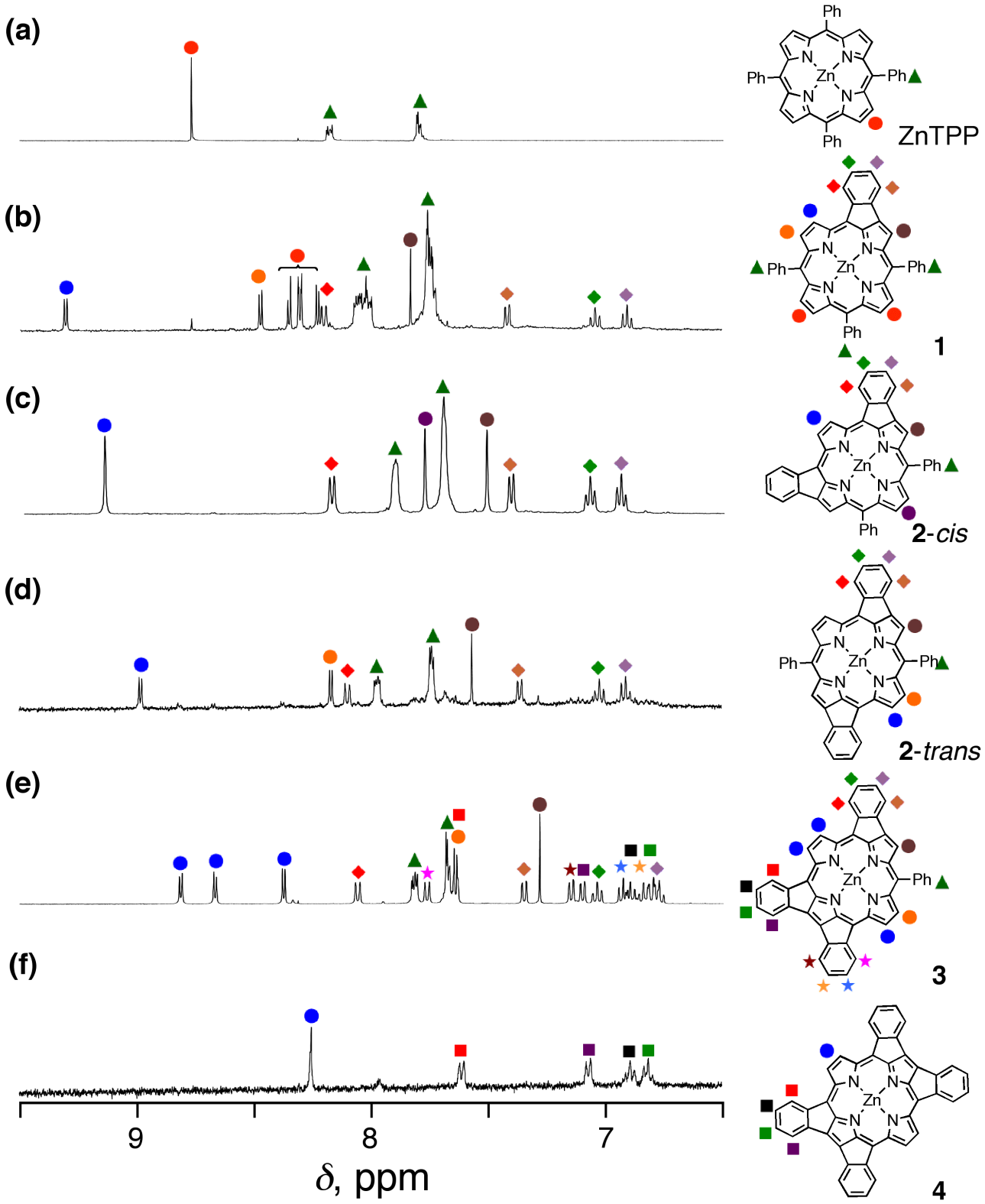

Fig. S1 ^{1}H NMR spectra of the fused porphyrins in DMSO-d_6 at 298 K; (a) ZnTPP, (b) **1**, (c) **2**-*cis*, (d) **2**-*trans*, (e) **3**, and (f) **4**.

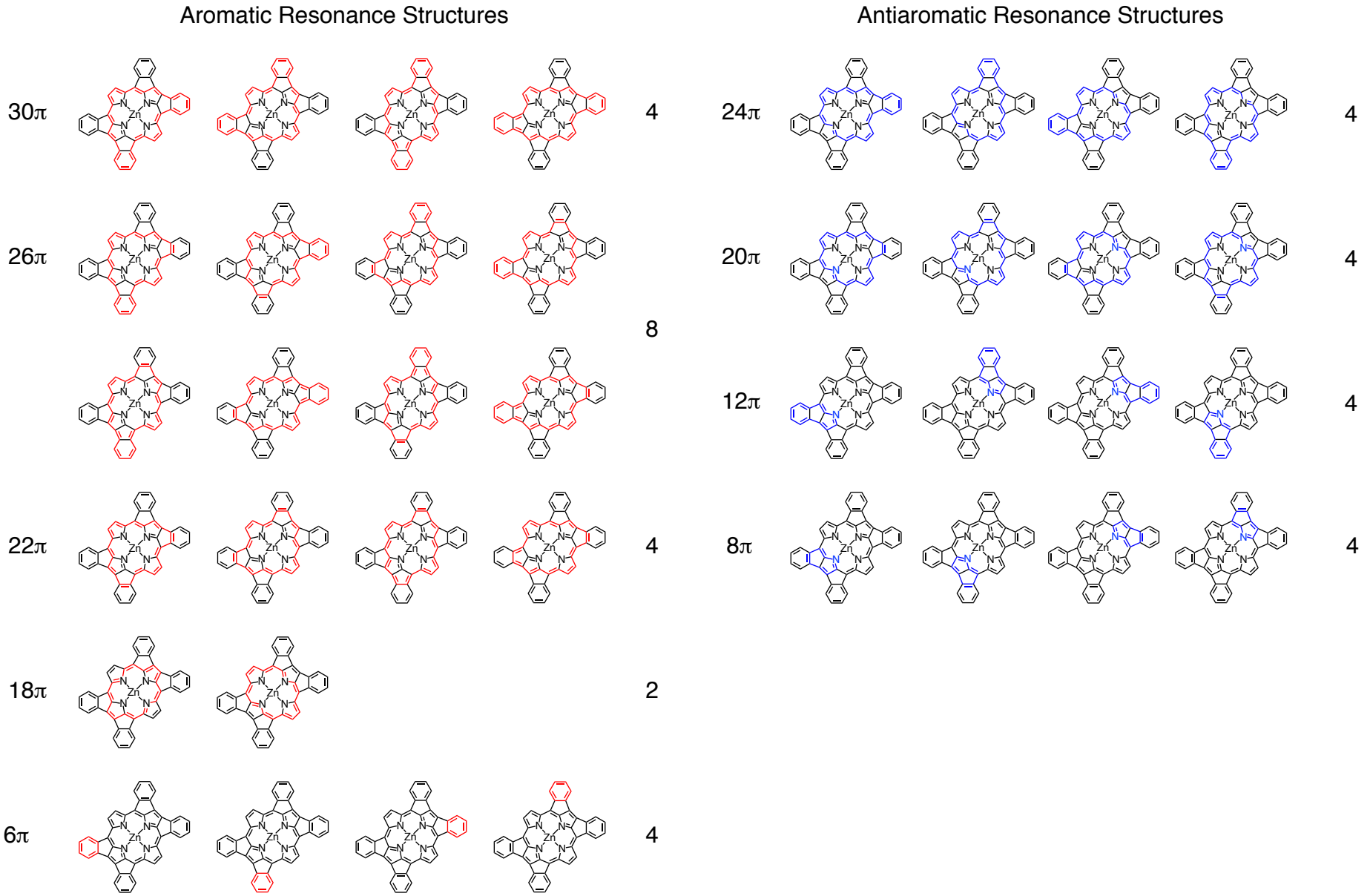

Fig. S2 Possible resonance structures of **4** having different aromatic circuits.

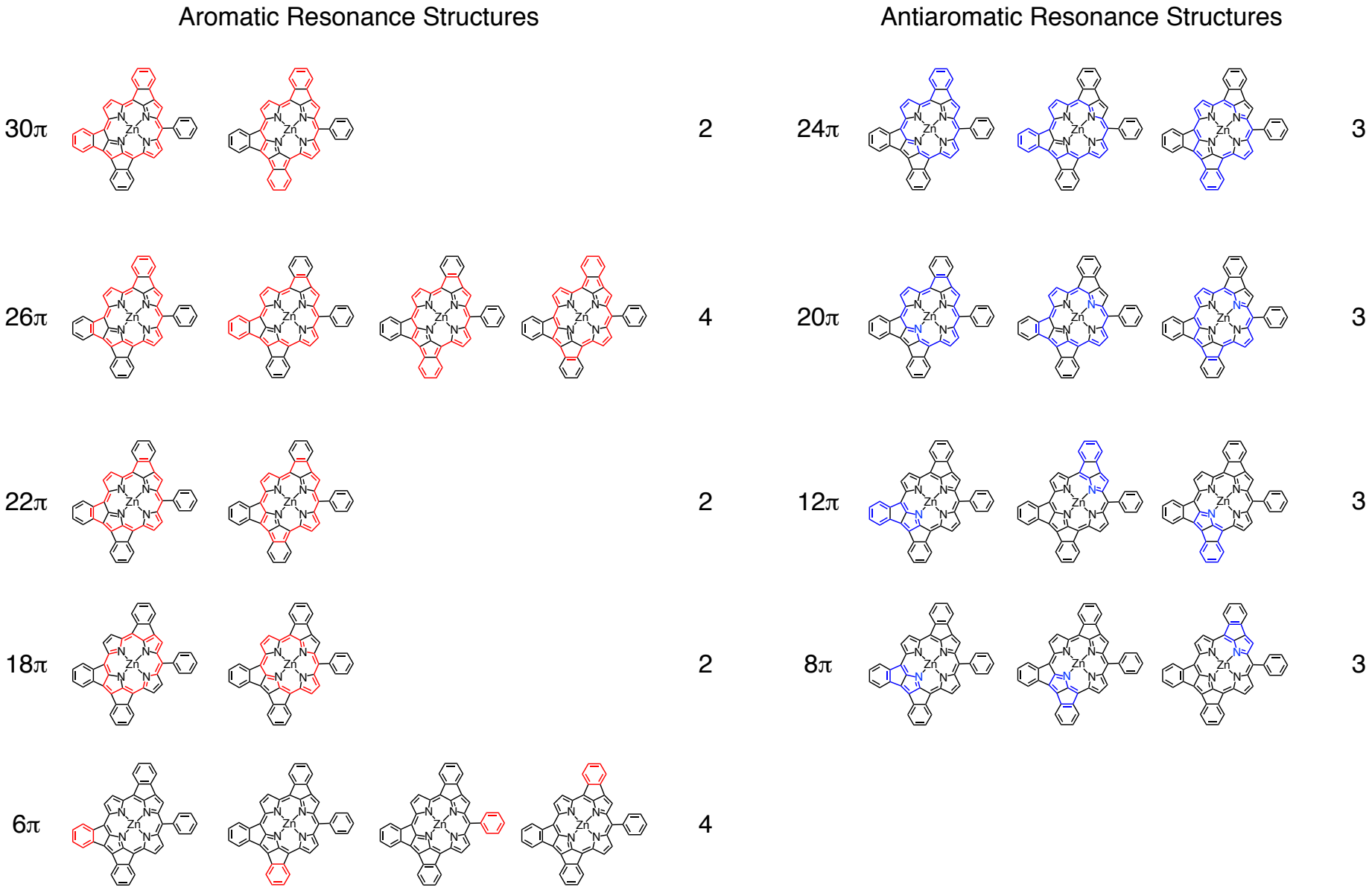

Fig. S3 Possible resonance structures of **3** having different aromatic circuits.

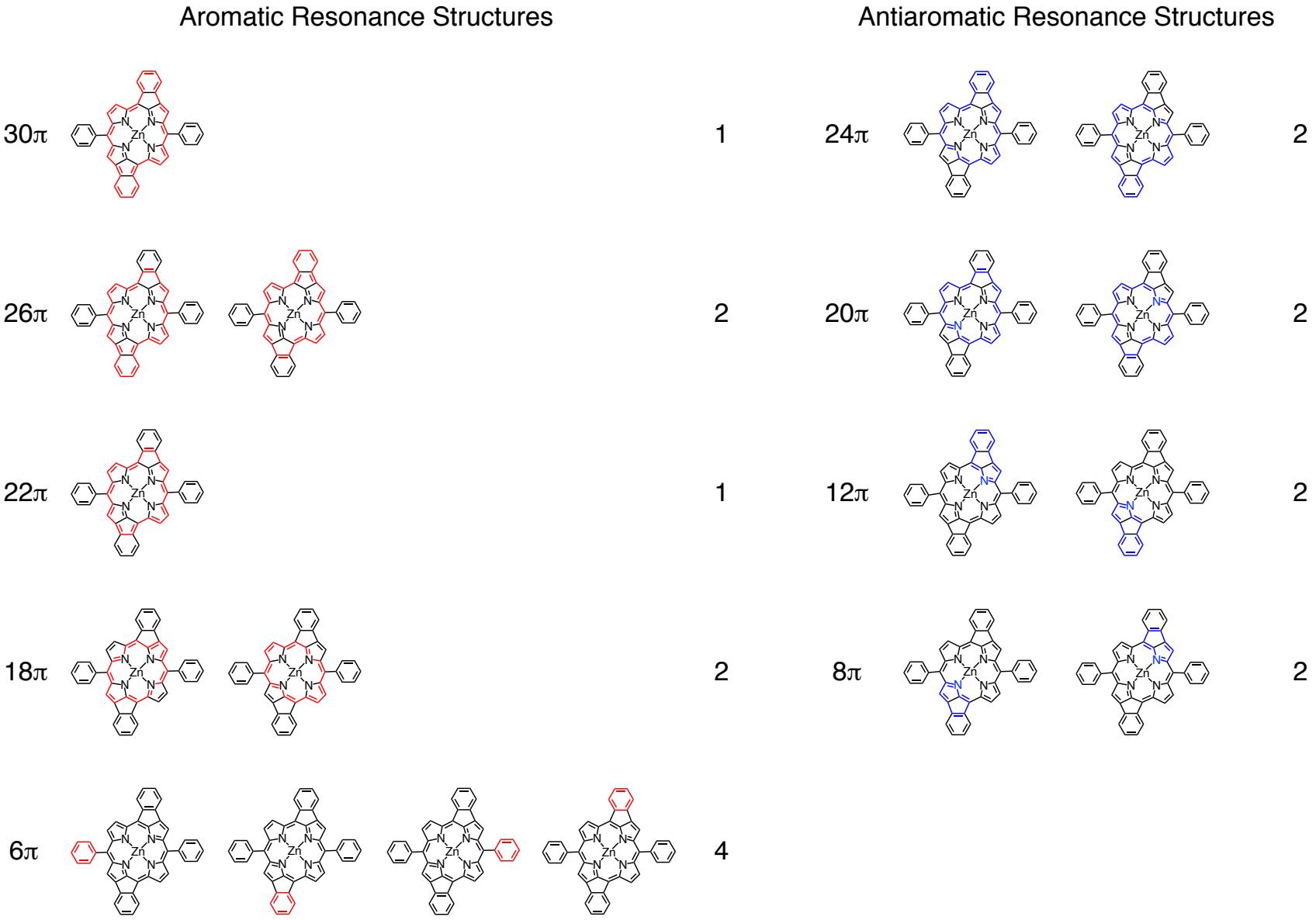

Fig. S4 Possible resonance structures of **2**-*trans* having different aromatic circuits.

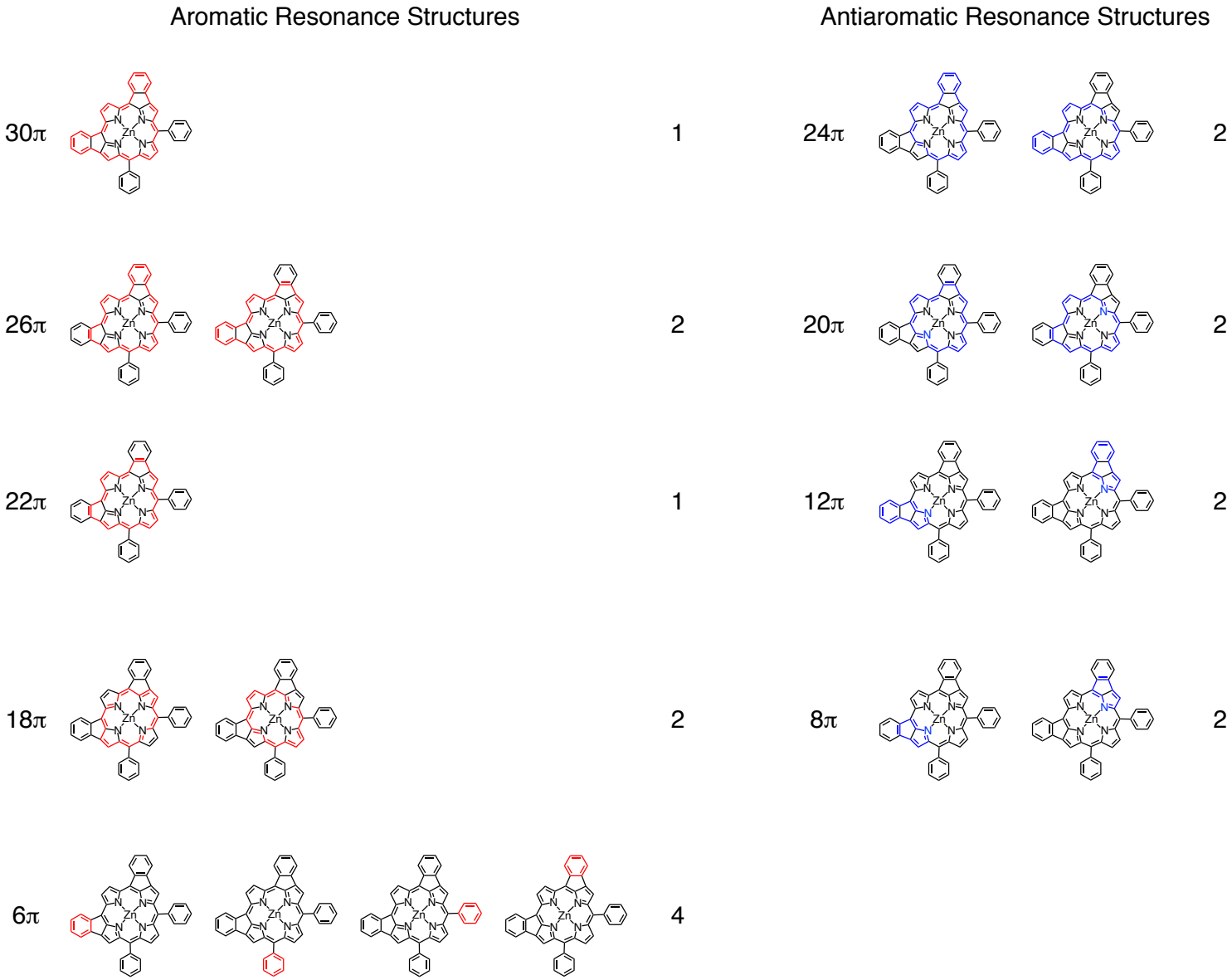

Fig. S5 Possible resonance structures of **2**-*cis* having different aromatic circuits.

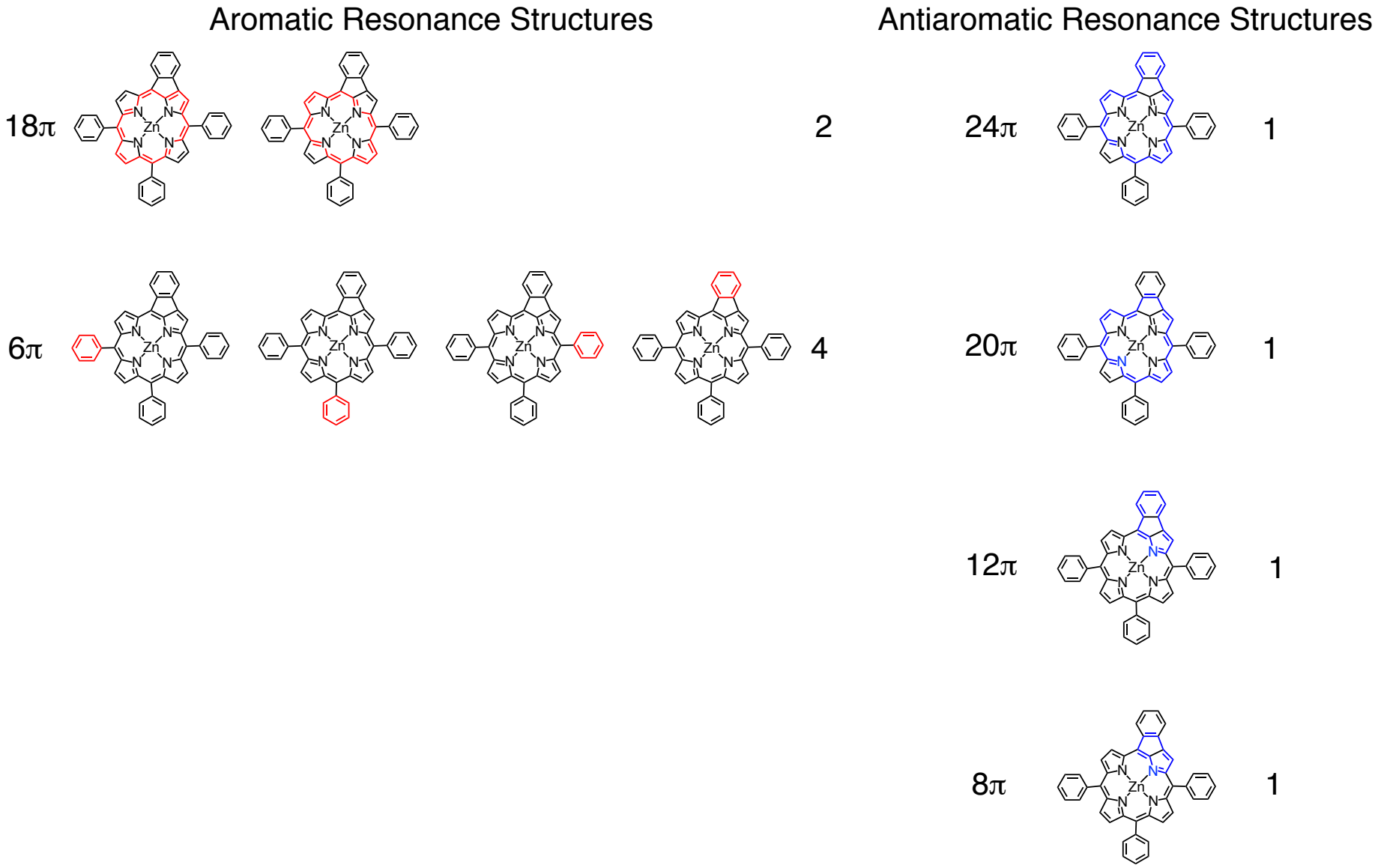

Fig. S6 Possible resonance structures of **1** having different aromatic circuits.

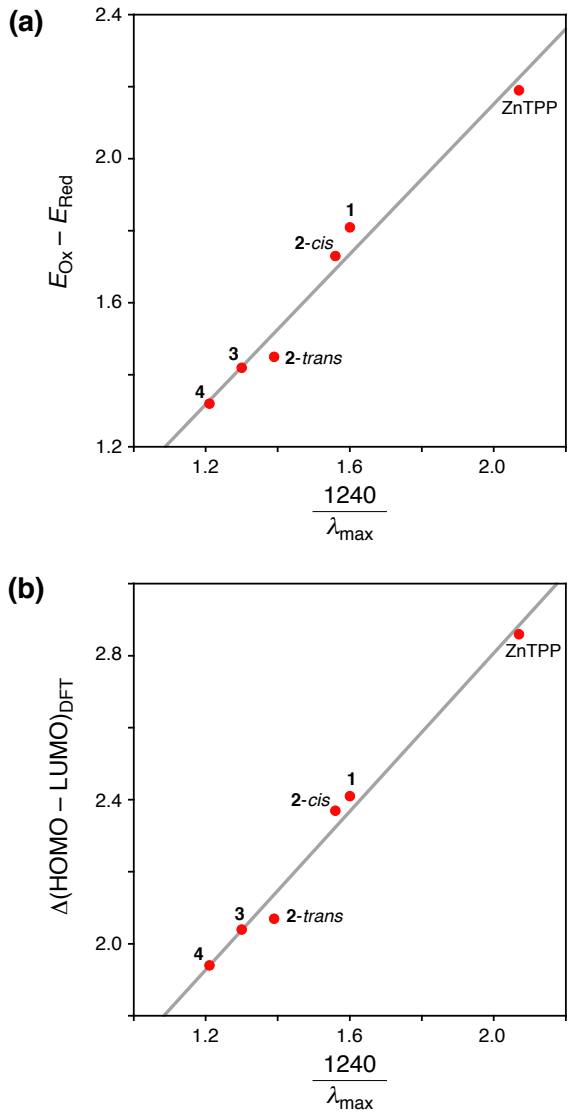

Fig. S7 Plots of HOMO-LUMO gaps obtained from the electrochemical measurements and DFT calculations against that obtained from the longest wavelengths of absorption maxima. As the HOMO-LUMO gaps obtained from the electrochemical studies were used the differences of the first oxidation and reduction potentials, and the HOMO-LUMO gaps obtained from the UV-vis absorption spectra were calculated as $1240/\lambda_{max}$, where λ_{max} stands for the wavelength (nm) of the lowest-energy absorption band of each compound.

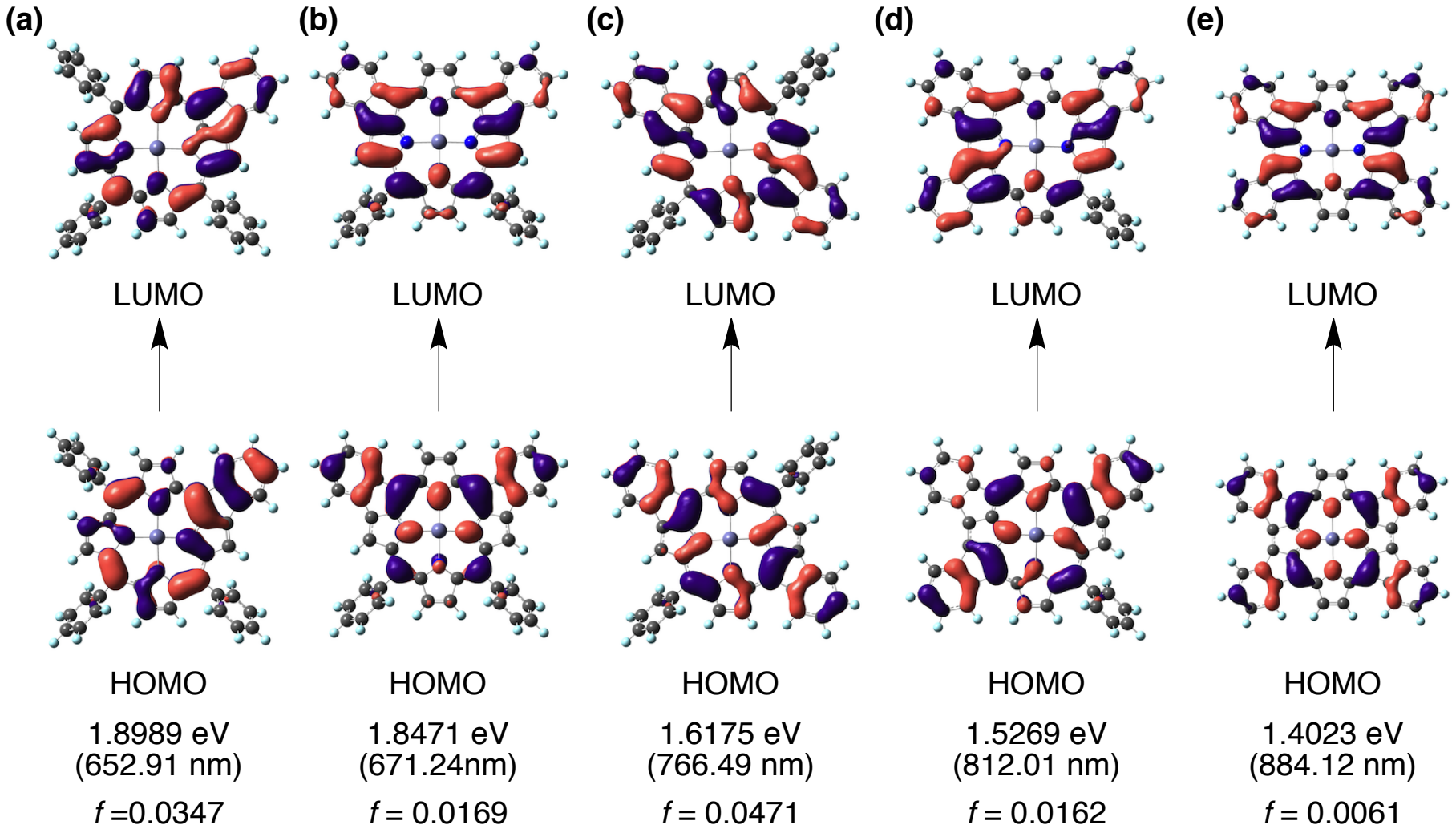

Fig. S8 The frontier orbitals related to the lowest-energy absorption bands with the transition energies and oscillator strengths (*f*) for **1** (a), **2**-*cis* (b), **2**-*trans* (c), **3** (d) and **4** (e), obtained from TD-DFT calculations at the B3LYP/6-31G(d) level of theory.

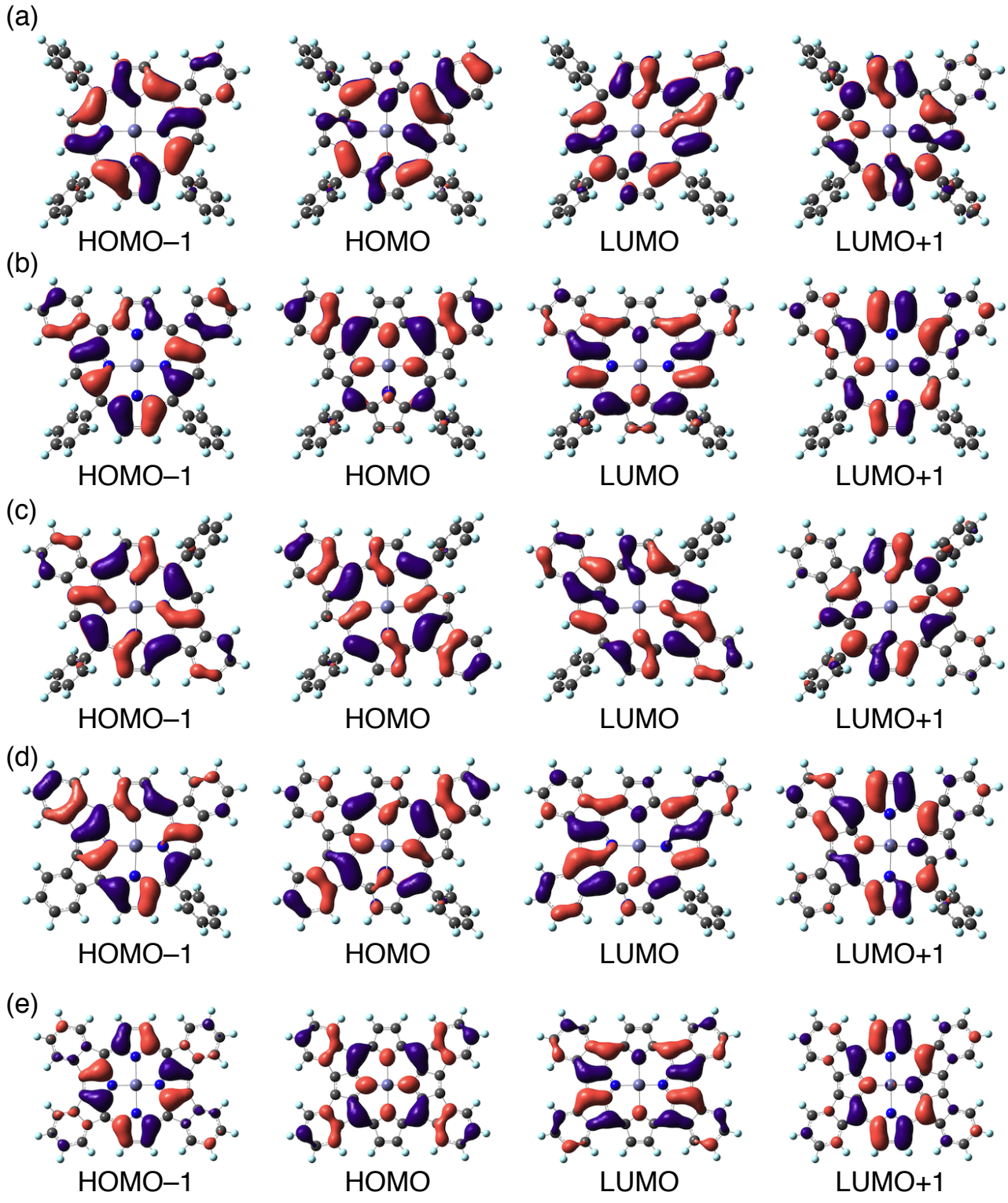

Fig. S9 The frontier four orbitals of **1** (a), **2**-*cis* (b), **2**-*trans* (c), **3** (d) and **4** (d), obtained from DFT calculations at the B3LYP/6-31G(d) level of theory.

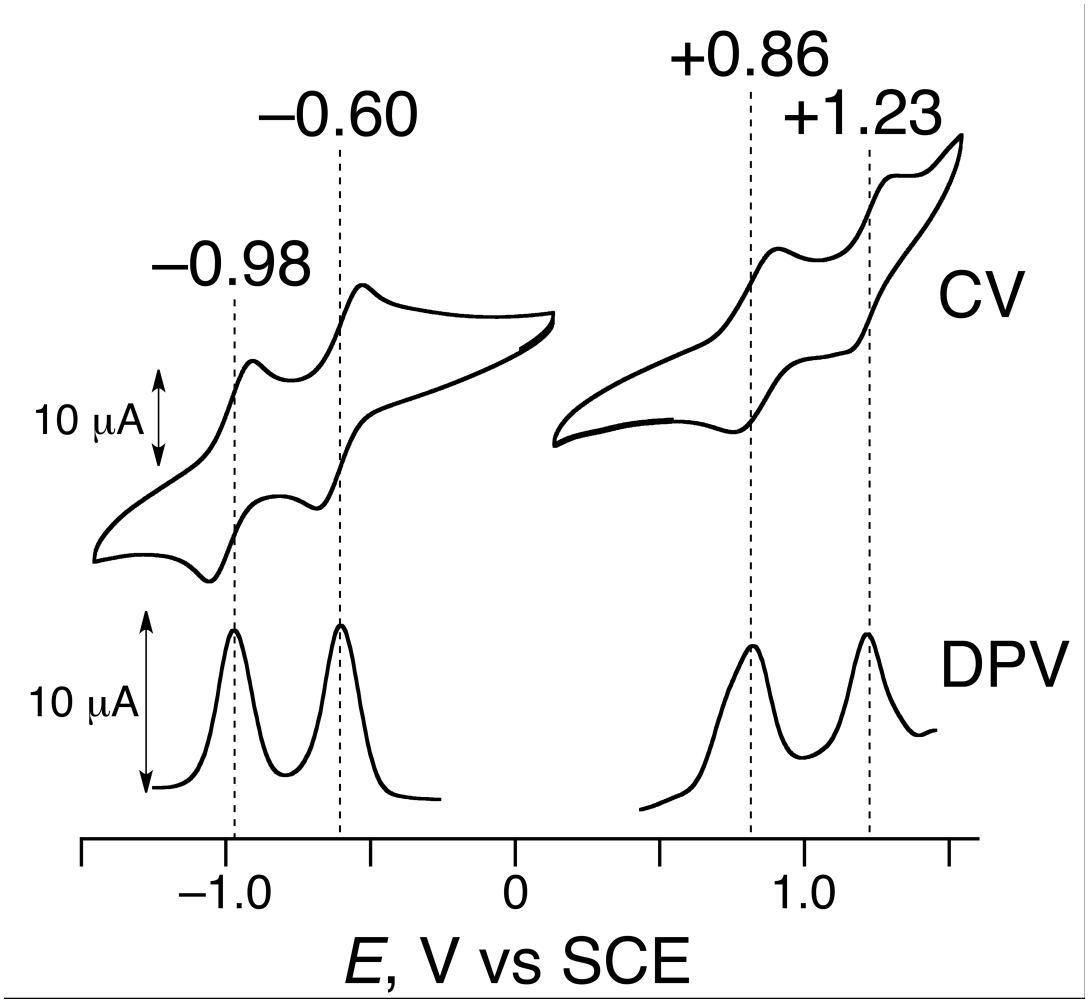

Fig. S10 Cyclic (above) and differential-pulse (below) voltammograms of **9** in THF at room temperature in the presence of $[(n\text{-Bu})_4\text{N}](\text{PF}_6)$ (0.1 M) as an electrolyte.

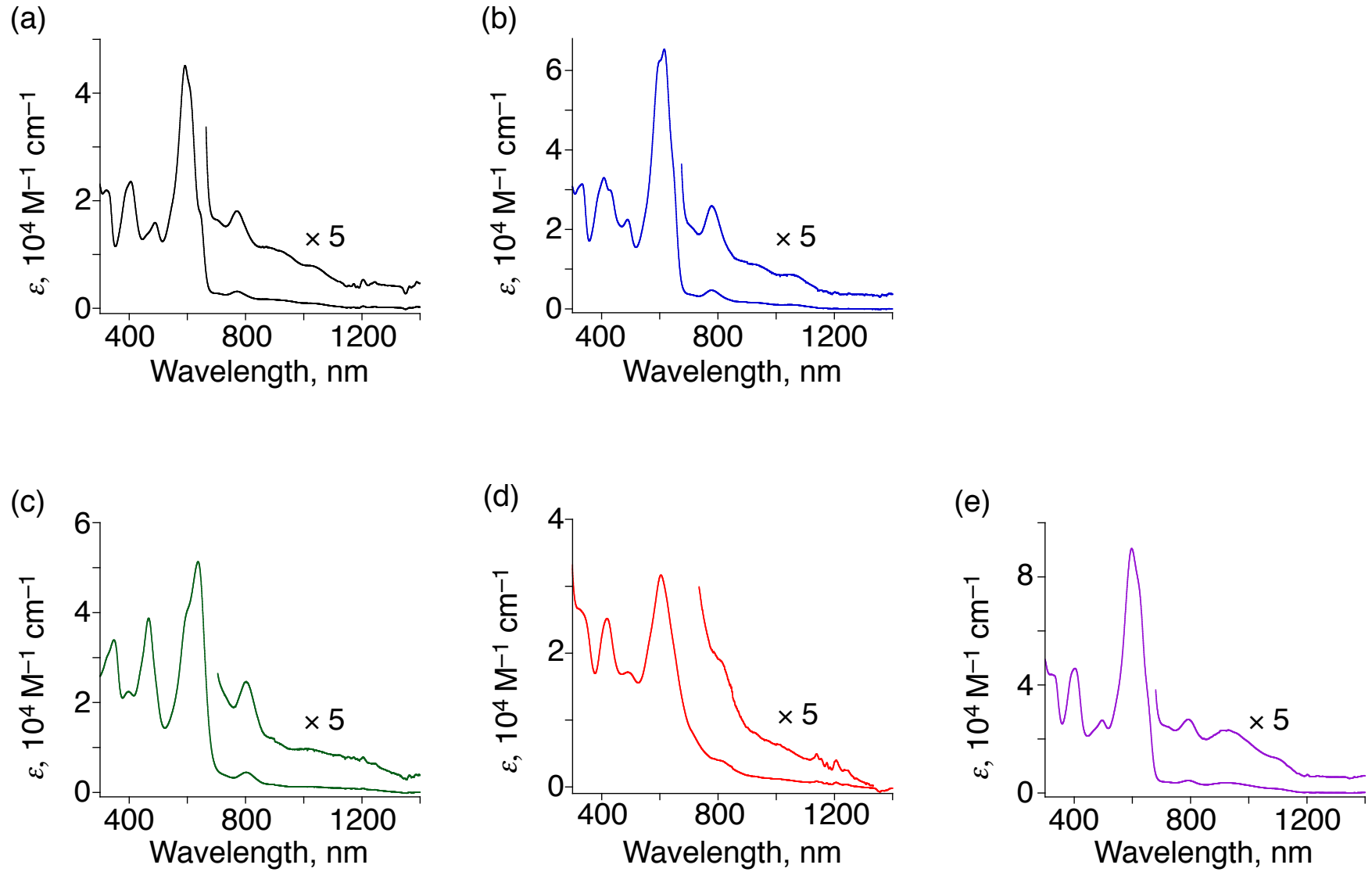

Fig. S11 UV-Vis spectra of the ZnQFP derivatives in DMF at 298 K; (a) **4**, (b) **5**, (c) **6**, (d) **7**, and (e) **8**.

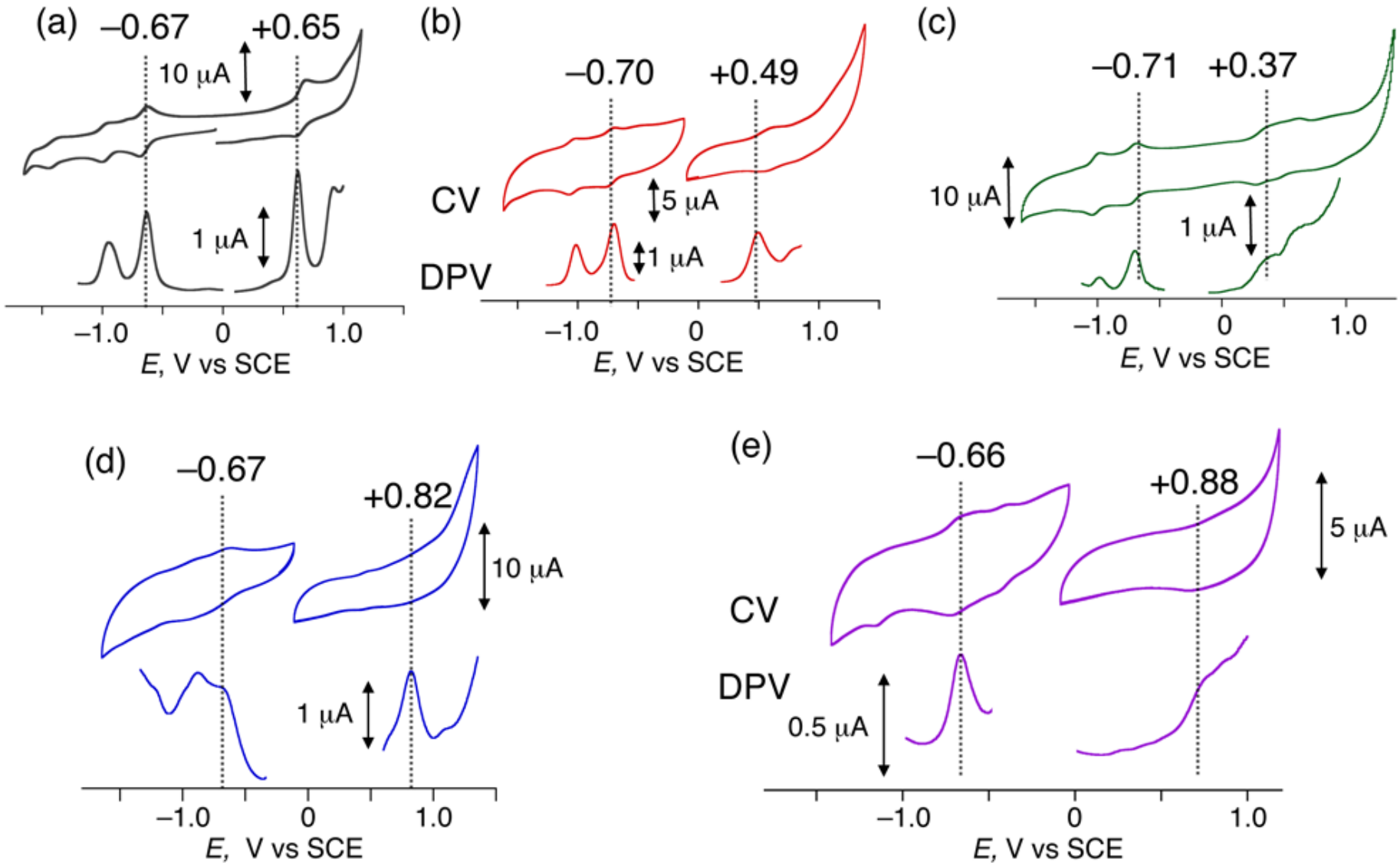

Fig. S12 Cyclic (above) and differential-pulse (below) voltammograms of the ZnQFP derivatives in DMF containing 0.1 M $TBAPF_6$ as an electrolyte at room temperature: (a) **4**, (b) **5**, (c) **6**, (d) **7**, and (e) **8**.

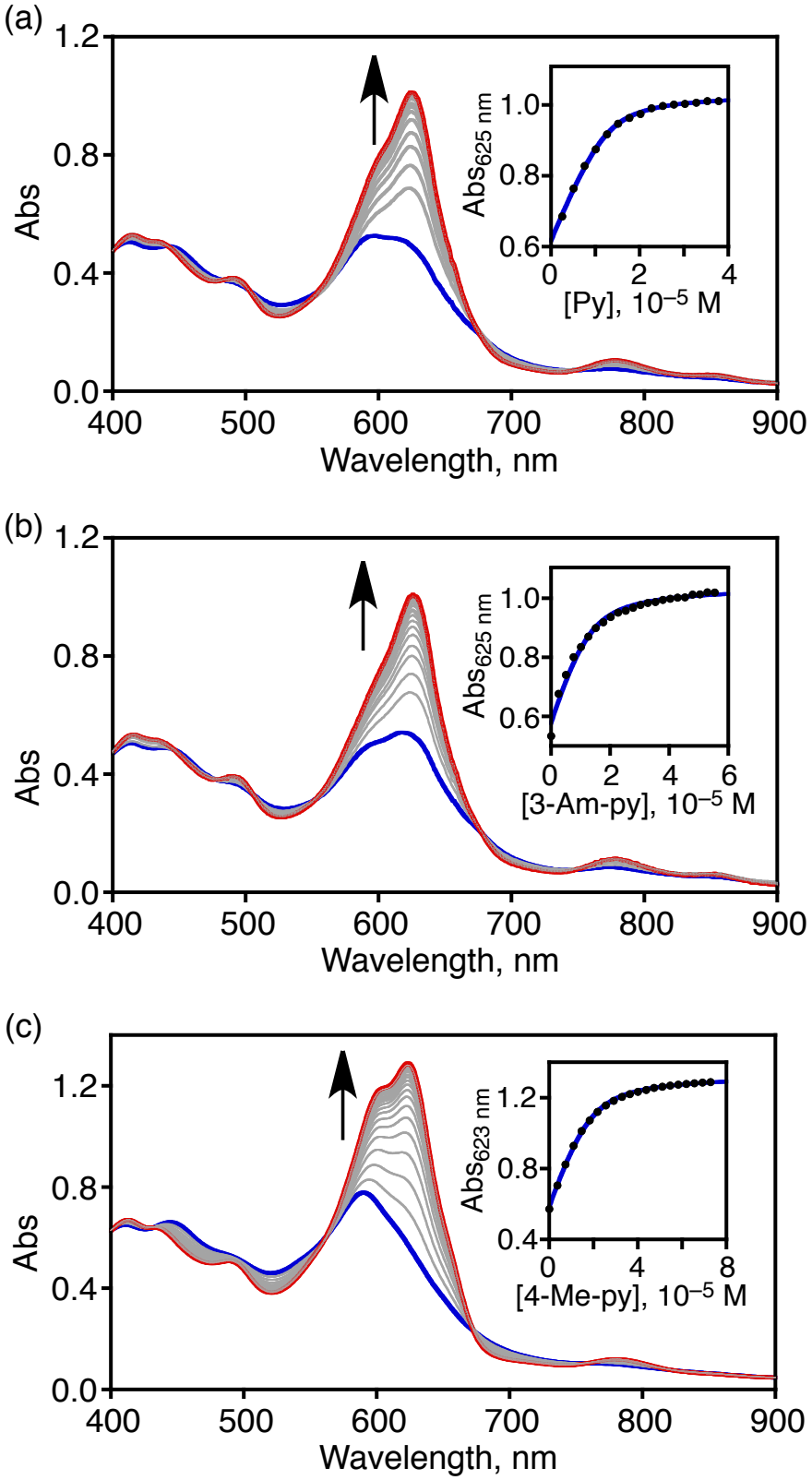

Fig. S13 UV-Vis spectral changes upon titration of **9** with py (a), 3-Am-py (b), and 4-Me-py (c) in CH_2Cl_2 at 298 K. Inset: the absorbance changes at 625 nm for (a) and (c), 623 nm for (b), fitted with eq S1. The concentrations of **9** were 1.26×10^{-5} M for (a) and (c), and 1.82×10^{-5} M for (b).

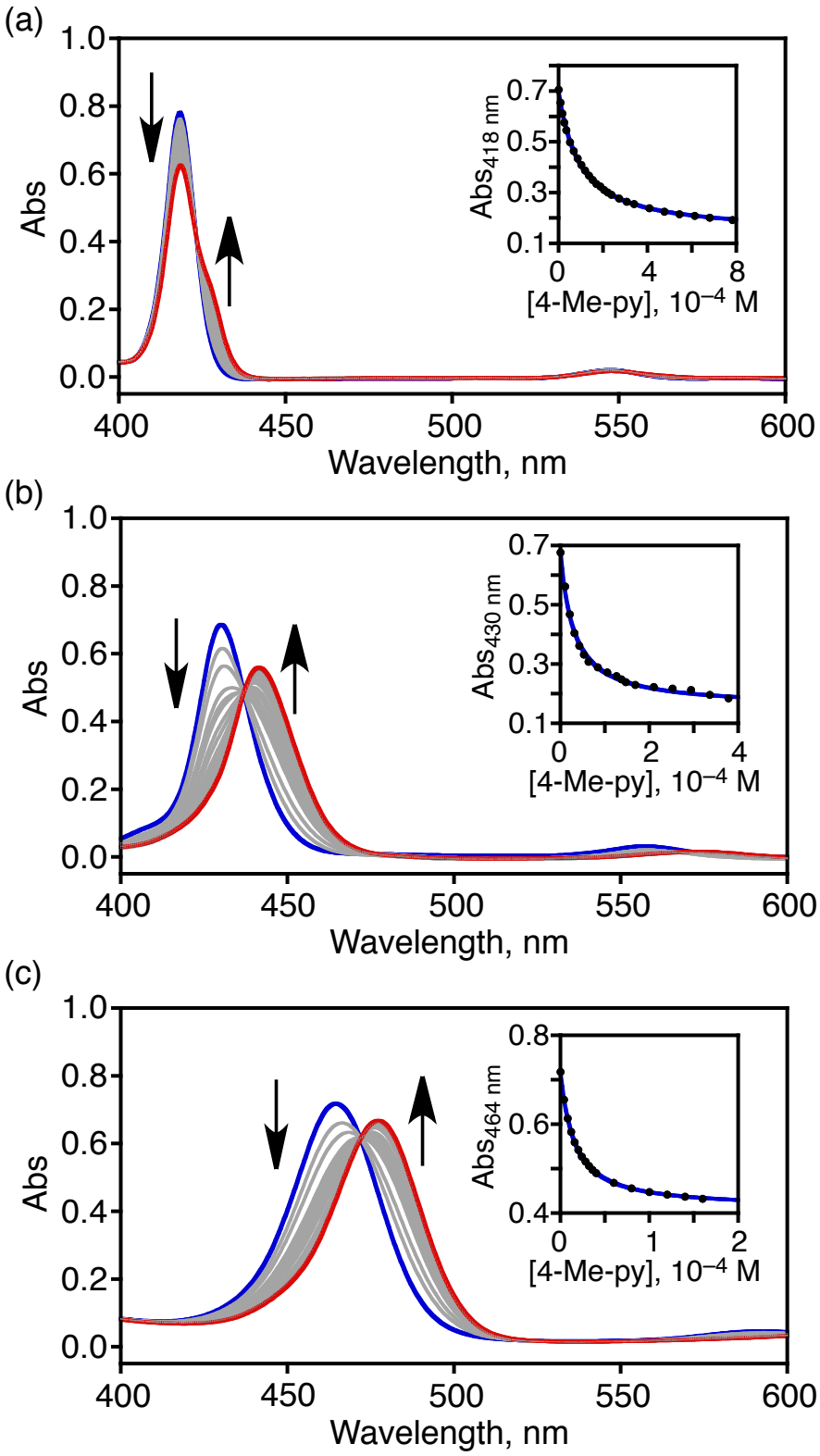

Fig. S14 UV-Vis spectral changes upon titration of ZnTPP (a), ZnOPP (b) and ZnDPP (c) with 4-Me-py in CH_2Cl_2 at 298 K. Inset: the absorbance changes at 418 nm for (a), 430 nm for (b), 464 nm for (c) fitted with eq S1. The concentrations of porphyrin derivatives were 1.82×10^{-6} M for (a), 2.1×10^{-6} M for (b), and 4.1×10^{-6} M for (c).

Table S1 Summary for the numbers of possible resonance structures having different aromatic and antiaromatic circuits for the fused porphyrin derivatives

Number of π-electrons	**1**	**2**-*cis*	**2**-*trans*	**3**	**4**
	Aromatic and antiaromatic circuits with the whole porphyrin structure				
18π	2	2	2	2	2
20π	1	2	2	3	4
22π	—	1	1	2	4
24π	1	2	2	3	4
26π	—	2	2	4	8
30π	—	1	1	2	4
	Aromatic and antiaromatic circuits with the partial structure				
6π	4	4	4	4	4
8π	1	2	2	3	4
12π	1	2	2	3	4

Table S2 Summary of oscillation strengths, HOMO-LUMO gaps obtained from the UV-Vis spectroscopy, electrochemical studies and DFT calculations for the ring-fused porphyrins.

	Oscillator Strength			Δ(HOMO – LUMO), eV		
	Soret	Q	total	CV [a]	UV-Vis-NIR [b]	DFT
ZnTPP	1.497 (389 – 444 nm) [c]	0.123 (497 – 647 nm) [c]	1.620	2.19	2.07	2.86
1	1.110 (430 – 538 nm) [c]	0.103 (540 – 821 nm) [c]	1.213	1.81	1.60	2.41
2-*cis*	0.884 (374 – 475 nm) [c]	0.077 (621 – 851 nm) [c]	0.961	1.73	1.56	2.37
2-*trans*	1.149 (445 – 614 nm) [c]	0.128 (615 – 967 nm) [c]	1.277	1.45	1.39	2.07
3	0.568 (389 – 444 nm) [c]	0.059 (389 – 444 nm) [c]	0.627	1.42	1.30	2.04
4	0.499 (389 – 444 nm) [c]	0.039 (389 – 444 nm) [c]	0.538	1.32	1.21	1.94

[a] Obtained from the difference between the first oxidation and first reduction potentials. [b] Obtained from the wavelength of the lowest absorption band. [c] The oscillator strength was calculated with the wavelength range indicated in the parenthesis.

Table S3 TD-DFT results for low-energy π-π* states of the ring-fused porphyrin derivatives[a]

compound	wavelength, nm	oscillator strength	contribution (weight %)[b]
1	652.91	0.0347	H→L (85), H–1→L+1 (10)
	476.70	0.0982	H–1→L+1 (43), H–2→L (39), H→L+1 (6)
	425.07	0.8041	H–1→L (33), H→L+1 (28), H–2→L+1 (18)
2-*cis*	674.00	0.0032	H–1→L (55), H→L+1 (44)
	671.24	0.0169	H→L (82), H–1→L+1 (16)
	567.23	0.0760	H–1→L+1 (73), H–2→L (10), H→L (10)
	484.07	0.6550	H→L+1 (43), H–1→L (33), H–3→L (18)
2-*trans*	766.49	0.0471	H→L (90), H–1→L+1 (6)
	480.73	0.2510	H–1→L+1 (41), H–3→L (29), H–1→L (16)
	443.79	0.5036	H–4→L (39), H–4→L+1 (18), H→L+1 (14)
	429.24	0. 7010	H–4→L (51), H–1→L (15)
3	812.01	0.0162	H→L (92), H–1→L+1 (5)
	590.67	0.0310	H–1→L+1 (66), H–2→L (10), H–3→L (9)
	518.38	0.6563	H→L+1 (33), H–2→L+2 (26), H–1→L (21)
	407.17	0.4693	H–5→L+1 (33), H–4→L (32), H–1→L+2 (13)
4	884.12	0.0061	H→L (94)
	818.53	0.0056	H–1→L (70), H→L+1 (29)
	534.38	0.9019	H→L+1 (64), H–1→L (26)
	461.65	0.3157	H–4→L (79), H–1→L+1 (8), H–2→L+2 (8)
	402.97	0.5580	H–6→L (67), H–3→L+2 (22)

[a] At the B3LYP/6-31G(d) level of theory. [b] H = HOMO, L = LUMO.

Table S4 Crystallographic data for QFP derivatives

compound	**5**-py	**5**-dox	**8**-py
crystal system	monoclinic	monoclinic	triclinic
space group	$P2_1/a$	$P2_1/a$	$P\ \bar{1}$
T, K		120	
$C_{60}H_{52}N_4Zn{\cdot}C_5H_5N{\cdot}2C_6H_5Cl$	$C_{60}H_{52}N_4Zn{\cdot}C_4H_8O_2$	$C_{48}H_{16}N_4F_{12}Zn{\cdot}C_5H_5N$	$C_{60}H_{52}N_4Zn{\cdot}C_5H_5N{\cdot}2C_6H_5Cl$
FW	1198.62	1130.72	1021.12
a, Å	17.737(2)	19.126(2)	16.724(13)
b, Å	18.295(3)	17.2247(18)	16.971(14)
c, Å	19.069(3)	19.215 (2)	20.045(16)
α, °	90	90	107.054(11)
β, °	92.168(2)	93.303(2)	107.580(10)
γ, °	90	90	105.011(12)
V, Å^3	6183.5(15)	6319.6(11)	4793(7)
Z	4	4	4
λ, Å		0.71073 (Mo Kα)	
D_c, g cm^{-3}	1.288	1.188	1.415
reflns measured	34682	33306	18428
reflns unique	13927	13857	12549
$R1$ ($I > 2\sigma(I)$)	0.0331	0.1176	0.0835
$wR2$ (all)	0.0916	0.3252	0.2096
GOF	1.038	1.137	0.838

Table S5 Cartesian coordinates of **1** calculated at the B3LYP/6-31G(d) level of theory

Atom	Coordinates (Angstroms) X	Y	Z
Zn	0.1119	–0.1019	–0.0136
N	0.5805	–2.1436	–0.0287
N	–1.8279	–0.5313	–0.0726
N	–0.4433	1.8912	0.0458
N	2.0451	0.3817	–0.0111
C	1.8568	–2.6511	0.0105
C	1.8014	–4.0996	0.0702
H	2.6586	–4.7548	0.1258
C	0.4875	–4.4517	0.0561
H	0.0817	–5.4519	0.0967
C	–0.2761	–3.2282	–0.0072
C	–1.6651	–3.0629	–0.0302
C	–2.2743	–1.8012	–0.0511
C	–3.7031	–1.8834	–0.0029
C	–4.1552	–0.591	0.0179
C	–2.9636	0.2587	–0.031
C	–2.9225	1.6587	–0.0062
C	–1.7181	2.409	0.0012
C	–1.6493	3.8481	–0.0896
H	–2.499	4.5113	–0.163
C	–0.3285	4.1881	–0.0969
H	0.0968	5.1782	–0.1741
C	0.421	2.9578	–0.0089
C	1.8294	2.8616	–0.0202
C	2.5658	1.6624	–0.014
C	4.0074	1.5874	0.0057
H	4.6752	2.4361	0.0193
C	4.3437	0.2679	0.0083
H	5.3358	–0.1589	0.0123
C	3.1129	–0.4867	0.0077
C	3.0429	–1.8974	0.0185
C	–2.8006	–4.0353	0.0037
C	–4.0394	–3.3103	0.0252
C	–5.2536	–3.9778	0.0612
H	–6.1872	–3.4217	0.0783
C	–5.2639	–5.3823	0.0741
H	–6.2109	–5.9142	0.1023
C	–4.0671	–6.0922	0.049
H	–4.0826	–7.1788	0.0563
C	–2.8305	–5.4243	0.0129
H	–1.9173	–6.0087	–0.0116
C	–4.2191	2.4025	0.0053
C	–4.5747	3.2106	1.0976
H	–3.8961	3.2888	1.9422
C	–5.7889	3.8972	1.1119

H	–6.049	4.5123	1.9694
C	–6.669	3.7904	0.0332
H	–7.6144	4.3263	0.044
C	–6.327	2.9917	–1.0593
H	–7.0028	2.9072	–1.9063
C	–5.1136	2.303	–1.0727
H	–4.8454	1.6905	–1.9289
C	2.6014	4.1459	–0.051
C	3.3359	4.5165	–1.1883
H	3.3375	3.8612	–2.0549
C	4.0501	5.7149	–1.2171
H	4.6087	5.9874	–2.1088
C	4.0432	6.5628	–0.108
H	4.6001	7.4957	–0.1298
C	3.3161	6.2055	1.0291
H	3.3081	6.8576	1.8985
C	2.5999	5.0082	1.0565
H	2.0384	4.7302	1.9441
C	4.3397	–2.6509	0.0438
C	4.7748	–3.3635	–1.0842
H	4.1644	–3.3562	–1.9831
C	5.9784	–4.0697	–1.0621
H	6.3006	–4.6126	–1.9468
C	6.7674	–4.0751	0.0895
H	7.7046	–4.625	0.1074
C	6.3456	–3.3699	1.2183
H	6.9514	–3.3722	2.1207
C	5.1422	–2.6638	1.1952
H	4.8131	–2.1207	2.0769
H	–5.169	–0.2209	0.0762

Table S6 Cartesian coordinates of **2**-*cis* calculated at the B3LYP/6-31G(d) level of theory

Atom	Coordinates (Angstroms) X	Y	Z
Zn	0.2453	–0.0268	0
N	2.3983	–0.0343	0
N	0.2022	–0.0827	–1.9435
N	–1.8356	0.0532	0
N	0.2022	–0.0827	1.9435
C	3.221	–0.0178	1.1068
C	4.606	0.0148	0.68
H	5.4707	0.0356	1.327
C	4.606	0.0148	–0.68
H	5.4707	0.0356	–1.327
C	3.221	–0.0178	–1.1068
C	2.7041	–0.0267	–2.4072
C	1.3237	–0.0477	–2.6845
C	1.046	0.0094	–4.0876
C	–0.3198	0.0239	–4.2057
H	–0.9269	0.0859	–5.0977
C	–0.8527	–0.0373	–2.845
C	–2.2005	–0.0186	–2.4581
C	–2.6485	–0.0104	–1.1057
C	–4.0227	–0.1213	–0.6837
H	–4.8769	–0.2139	–1.3388
C	–4.0227	–0.1213	0.6837
H	–4.8769	–0.2139	1.3388
C	–2.6485	–0.0104	1.1057
C	–2.2005	–0.0186	2.4581
C	–0.8527	–0.0373	2.845
C	–0.3198	0.0239	4.2057
H	–0.9269	0.0859	5.0977
C	1.046	0.0094	4.0876
C	1.3237	–0.0477	2.6845
C	2.7041	–0.0267	2.4072
C	3.3558	0.0206	–3.7515
C	2.3425	0.0467	–4.7685
C	2.683	0.095	–6.1122
H	1.9095	0.1155	–6.8753
C	4.0386	0.1159	–6.4754
H	4.3152	0.1531	–7.5254
C	5.0274	0.0881	–5.4953
H	6.075	0.1027	–5.7839
C	4.6929	0.0405	–4.1317
H	5.4893	0.0175	–3.3961
C	–3.237	–0.0156	–3.5349
C	–4.1334	1.0578	–3.6658
H	–4.0632	1.8941	–2.9763
C	–5.0958	1.0637	–4.6753

H	–5.7754	1.907	–4.7655
C	–5.1832	–0.0055	–5.5692
H	–5.9346	–0.0014	–6.3542
C	–4.3005	–1.0801	–5.4477
H	–4.3653	–1.9199	–6.1344
C	–3.3348	–1.0845	–4.4407
H	–2.6556	–1.9264	–4.3421
C	–3.237	–0.0156	3.5349
C	–3.3348	–1.0845	4.4407
H	–2.6556	–1.9264	4.3421
C	–4.3005	–1.0801	5.4477
H	–4.3653	–1.9199	6.1344
C	–5.1832	–0.0055	5.5692
H	–5.9346	–0.0014	6.3542
C	–5.0958	1.0637	4.6753
H	–5.7754	1.907	4.7655
C	–4.1334	1.0578	3.6658
H	–4.0632	1.8941	2.9763
C	3.3558	0.0206	3.7515
C	2.3425	0.0467	4.7685
C	2.683	0.095	6.1122
H	1.9095	0.1155	6.8753
C	4.0386	0.1159	6.4754
H	4.3152	0.1531	7.5254
C	5.0274	0.0881	5.4953
H	6.075	0.1027	5.7839
C	4.6929	0.0405	4.1317
H	5.4893	0.0175	3.3961

Table S7 Cartesian coordinates of **2**-*trans* calculated at the B3LYP/6-31G(d) level of theory

Atom	Coordinates (Angstroms)		
	X	Y	Z
Zn	0	0	0.0108
N	–1.4864	1.5076	–0.0119
N	1.4311	1.3147	0.0679
N	1.4864	–1.5076	–0.0119
N	–1.4311	–1.3147	0.0679
C	–2.8429	1.2927	0.022
C	–3.5271	2.5692	0.0744
H	–4.5978	2.7032	0.1307
C	–2.5715	3.5423	0.0583
H	–2.7328	4.6097	0.1
C	–1.2948	2.8735	0.0088
C	0	3.4185	0.003
C	1.1642	2.6378	0.0284
C	2.3568	3.4268	–0.0077
C	3.4022	2.5406	–0.0033
C	2.8078	1.2031	0.0465
C	3.4869	–0.0289	0.0357
C	2.8429	–1.2927	0.022
C	3.5271	–2.5692	0.0744
H	4.5978	–2.7032	0.1307
C	2.5715	–3.5423	0.0583
H	2.7328	–4.6097	0.1
C	1.2948	–2.8735	0.0088
C	0	–3.4185	0.003
C	–1.1642	–2.6378	0.0284
C	–2.3568	–3.4268	–0.0077
C	–3.4022	–2.5406	–0.0033
H	–4.4644	–2.7365	–0.041
C	–2.8078	–1.2031	0.0465
C	–3.4869	0.0289	0.0357
C	0.4931	4.8304	–0.042
C	1.9282	4.8295	–0.0493
C	2.6395	6.0177	–0.0932
H	3.7262	6.0095	–0.0993
C	1.9386	7.2352	–0.1318
H	2.4879	8.1719	–0.1659
C	0.5474	7.2438	–0.1291
H	0.0122	8.1889	–0.1619
C	–0.1831	6.0427	–0.0862
H	–1.2667	6.0842	–0.0929
C	4.9824	0.001	0.0351
C	5.6887	0.5305	1.1273
H	5.1361	0.9056	1.9841
C	7.0835	0.5651	1.1262
H	7.6122	0.9729	1.9837

C	7.7972	0.0727	0.032
H	8.8835	0.1002	0.0308
C	7.1069	–0.4552	–1.0607
H	7.6538	–0.8355	–1.9195
C	5.7122	–0.4914	–1.059
H	5.1777	–0.8938	–1.9148
C	–0.4931	–4.8304	–0.042
C	–1.9282	–4.8295	–0.0493
C	–2.6395	–6.0177	–0.0932
H	–3.7262	–6.0095	–0.0993
C	–1.9386	–7.2352	–0.1318
H	–2.4879	–8.1719	–0.1659
C	–0.5474	–7.2438	–0.1291
H	–0.0122	–8.1889	–0.1619
C	0.1831	–6.0427	–0.0862
H	1.2667	–6.0842	–0.0929
C	–4.9824	–0.001	0.0351
C	–5.7122	0.4914	–1.059
H	–5.1777	0.8938	–1.9148
C	–7.1069	0.4552	–1.0607
H	–7.6538	0.8355	–1.9195
C	–7.7972	–0.0727	0.032
H	–8.8835	–0.1002	0.0308
C	–7.0835	–0.5651	1.1262
H	–7.6122	–0.9729	1.9837
C	–5.6887	–0.5305	1.1273
H	–5.1361	–0.9056	1.9841
H	4.4644	2.7365	–0.041

Table S8 Cartesian coordinates of **3** calculated at the B3LYP/6-31G(d) level of theory

Atom	Coordinates (Angstroms) X	Y	Z
Zn	–0.0891	0.1192	0.0057
N	0.1728	2.2937	0.0226
N	1.7922	–0.0217	0.0425
N	–0.2127	–2.0059	–0.0228
N	–1.9774	0.243	0.0704
C	–0.8551	3.2076	0.0102
C	–0.3041	4.5492	–0.0032
H	–0.8662	5.4718	–0.0134
C	1.0542	4.4237	0.0042
H	1.7793	5.2259	–0.0009
C	1.3536	3.0069	0.0199
C	2.6056	2.3548	0.0291
C	2.7075	0.964	0.0366
C	4.0677	0.4651	0.0231
C	3.9419	–0.9166	0.0152
C	2.5167	–1.1629	0.0227
C	2.1647	–2.507	0.0079
C	0.8121	–2.9301	0.009
C	0.2544	–4.2569	0.0687
H	0.8124	–5.1818	0.1171
C	–1.1067	–4.1183	0.08
H	–1.8427	–4.9072	0.1415
C	–1.3943	–2.6996	0.0151
C	–2.6952	–2.1141	0.0235
C	–2.9624	–0.7297	0.0346
C	–4.2671	–0.0689	–0.0245
H	–5.2134	–0.5881	–0.0772
C	–4.0237	1.2824	–0.0182
C	–2.603	1.4369	0.0323
C	–2.1982	2.7875	0.0112
C	4.0302	2.8148	0.0189
C	4.9072	1.6694	0.0155
C	6.2837	1.838	0.0054
H	6.9427	0.9738	0.0025
C	6.82	3.1366	–0.001
H	7.8977	3.2732	–0.0087
C	5.9781	4.2441	0.003
H	6.4008	5.245	–0.0015
C	4.5799	4.0886	0.0129
H	3.948	4.971	0.0164
C	3.4827	–3.2205	–0.0068
C	4.5526	–2.2539	–0.0025
C	5.8739	–2.6695	–0.017
H	6.6799	–1.9406	–0.014
C	6.1642	–4.0459	–0.0366

H	7.1991	–4.3763	–0.0474
C	5.1357	–4.9809	–0.0438
H	5.3687	–6.042	–0.0609
C	3.788	–4.5723	–0.0303
H	3.0042	–5.3227	–0.0416
C	–3.8706	–3.0388	0.021
C	–4.101	–3.9078	–1.0581
H	–3.4168	–3.899	–1.9017
C	–5.2022	–4.7643	–1.0612
H	–5.3677	–5.4242	–1.9087
C	–6.0911	–4.7698	0.0154
H	–6.9481	–5.438	0.013
C	–5.8721	–3.9125	1.0951
H	–6.5549	–3.9144	1.9407
C	–4.7727	–3.0537	1.0974
H	–4.5993	–2.395	1.9436
C	–3.4826	3.5536	–0.0374
C	–4.5865	2.6357	–0.0585
C	–5.8935	3.0951	–0.1078
H	–6.7232	2.3935	–0.1246
C	–6.1334	4.4784	–0.136
H	–7.1545	4.8477	–0.1743
C	–5.0689	5.375	–0.1148
H	–5.2618	6.4442	–0.1362
C	–3.7404	4.9191	–0.0659
H	–2.9355	5.6455	–0.0506

Table S9 Cartesian coordinates of **4** calculated at the B3LYP/6-31G(d) level of theory

Atom	Coordinates (Angstroms) X	Y	Z
Zn	0	0	0
N	0	-2.1899	0
N	0	0	1.8453
N	0	2.1899	0
N	0	0	–1.8453
C	0	–3.0024	–1.1129
C	0	–4.3852	–0.6841
H	0	–5.2535	–1.3286
C	0	–4.3852	0.6841
H	0	–5.2535	1.3286
C	0	–3.0024	1.1129
C	0	–2.449	2.4209
C	0	–1.0734	2.6587
C	0	–0.6955	4.0557
C	0	0.6955	4.0557
C	0	1.0734	2.6587
C	0	2.449	2.4209
C	0	3.0024	1.1129
C	0	4.3852	0.6841
H	0	5.2535	1.3286
C	0	4.3852	–0.6841
H	0	5.2535	–1.3286
C	0	3.0024	–1.1129
C	0	2.449	–2.4209
C	0	1.0734	–2.6587
C	0	0.6955	–4.0557
C	0	–0.6955	–4.0557
C	0	–1.0734	–2.6587
C	0	–2.449	–2.4209
C	0	–3.0348	3.801
C	0	–1.9745	4.7806
C	0	–2.2707	6.1348
H	0	–1.4719	6.8716
C	0	–3.6143	6.5483
H	0	–3.85	7.6088
C	0	–4.6386	5.608
H	0	–5.6745	5.9358
C	0	–4.3535	4.2296
H	0	–5.1727	3.5179
C	0	3.0348	3.801
C	0	1.9745	4.7806
C	0	2.2707	6.1348
H	0	1.4719	6.8716
C	0	3.6143	6.5483
H	0	3.85	7.6088

C	0	4.6386	5.608
H	0	5.6745	5.9358
C	0	4.3535	4.2296
H	0	5.1727	3.5179
C	0	3.0348	–3.801
C	0	1.9745	–4.7806
C	0	2.2707	–6.1348
H	0	1.4719	–6.8716
C	0	3.6143	–6.5483
H	0	3.85	–7.6088
C	0	4.6386	–5.608
H	0	5.6745	–5.9358
C	0	4.3535	–4.2296
H	0	5.1727	–3.5179
C	0	–3.0348	–3.801
C	0	–1.9745	–4.7806
C	0	–2.2707	–6.1348
H	0	–1.4719	–6.8716
C	0	–3.6143	–6.5483
H	0	–3.85	–7.6088
C	0	–4.6386	–5.608
H	0	–5.6745	–5.9358
C	0	–4.3535	–4.2296
H	0	–5.1727	–3.5179

Table S10 Cartesian coordinates of $1e^-$-oxidized **4** calculated at the B3LYP/6-31G(d) level of theory

Atom	Coordinates (Angstroms) X	Y	Z
Zn	0.0004	0.0002	0
N	–1.9549	–0.9997	0
N	–0.845	1.6511	0
N	1.9549	0.9997	0
N	0.845	–1.6511	0
C	–2.1755	–2.3583	0
C	–3.5975	–2.6092	0
H	–4.0783	–3.5761	0
C	–4.2214	–1.3904	0
H	–5.287	–1.2153	0
C	–3.1863	–0.3835	0
C	–3.2876	1.0384	0
C	–2.1661	1.8849	0
C	–2.4682	3.2973	0
C	–1.229	3.9312	0
C	–0.2608	2.8594	0
C	1.0813	3.2728	0
C	2.1755	2.3583	0
C	3.5975	2.6091	0
H	4.0783	3.576	0
C	4.2214	1.3904	0
H	5.2869	1.2152	0
C	3.1862	0.3834	0
C	3.2876	–1.0385	0
C	2.1659	–1.885	0
C	2.4682	–3.2973	0
C	1.2289	–3.9312	0
C	0.2607	–2.8595	0
C	–1.0814	–3.2727	0
C	–4.4293	1.9907	0
C	–3.9356	3.3513	0
C	–4.8213	4.4162	0
H	–4.4566	5.4383	0
C	–6.2028	4.1589	0
H	–6.9012	4.9894	0
C	–6.684	2.8509	0
H	–7.7538	2.6703	0
C	–5.8011	1.7606	0
H	–6.2008	0.7533	0
C	0.9782	4.7559	0
C	–0.4136	5.1527	0
C	–0.7574	6.4945	0
H	–1.7994	6.7981	0
C	0.2607	7.4634	0

H	–0.0034	8.5159	0
C	1.6023	7.087	0
H	2.3757	7.848	0
C	1.9684	5.7324	0
H	3.0189	5.4661	0
C	4.4292	–1.9908	0
C	3.9355	–3.3513	0
C	4.8212	–4.4162	0
H	4.4564	–5.4384	0
C	6.2027	–4.1589	0
H	6.9011	–4.9895	0
C	6.6839	–2.851	0
H	7.7537	–2.6704	0
C	5.801	–1.7606	0
H	6.2007	–0.7534	0
C	–0.9782	–4.756	0
C	0.4135	–5.1528	0
C	0.7572	–6.4946	0
H	1.7992	–6.7983	0
C	–0.2608	–7.4635	0
H	0.0032	–8.516	0
C	–1.6025	–7.087	0
H	–2.3759	–7.8479	0
C	–1.9684	–5.7325	0
H	–3.019	–5.4662	0

Table S11 Cartesian coordinates of 1e$^-$-reduced **4** calculated at the B3LYP/6-31G(d) level of theory

Atom	Coordinates (Angstroms)		
	X	Y	Z
Zn	0	0	0
N	0	2.1981	0
N	0	0	1.8499
N	0	–2.1981	0
N	0	0	–1.8499
C	0	3.0095	–1.1163
C	0	4.3953	–0.6831
H	0	5.263	–1.3284
C	0	4.3953	0.6831
H	0	5.263	1.3284
C	0	3.0095	1.1163
C	0	2.4658	2.4203
C	0	1.0753	2.6672
C	0	0.7078	4.0488
C	0	–0.7078	4.0488
C	0	–1.0753	2.6672
C	0	–2.4658	2.4203
C	0	–3.0095	1.1163
C	0	–4.3953	0.6831
H	0	–5.263	1.3284
C	0	–4.3953	–0.6831
H	0	–5.263	–1.3284
C	0	–3.0095	–1.1163
C	0	–2.4658	–2.4203
C	0	–1.0753	–2.6672
C	0	–0.7078	–4.0488
C	0	0.7078	–4.0488
C	0	1.0753	–2.6672
C	0	2.4658	–2.4203
C	0	3.0485	3.7877
C	0	1.9788	4.7692
C	0	2.2842	6.1269
H	0	1.4851	6.8637
C	0	3.6243	6.5403
H	0	3.8594	7.6016
C	0	4.6544	5.6001
H	0	5.6899	5.9303
C	0	4.3686	4.2251
H	0	5.1871	3.5123
C	0	–3.0485	3.7877
C	0	–1.9788	4.7692
C	0	–2.2842	6.1269
H	0	–1.4851	6.8637
C	0	–3.6243	6.5403

H	0	–3.8594	7.6016
C	0	–4.6544	5.6001
H	0	–5.6899	5.9303
C	0	–4.3686	4.2251
H	0	–5.1871	3.5123
C	0	–3.0485	–3.7877
C	0	–1.9788	–4.7692
C	0	–2.2842	–6.1269
H	0	–1.4851	–6.8637
C	0	–3.6243	–6.5403
H	0	–3.8594	–7.6016
C	0	–4.6544	–5.6001
H	0	–5.6899	–5.9303
C	0	–4.3686	–4.2251
H	0	–5.1871	–3.5123
C	0	3.0485	–3.7877
C	0	1.9788	–4.7692
C	0	2.2842	–6.1269
H	0	1.4851	–6.8637
C	0	3.6243	–6.5403
H	0	3.8594	–7.6016
C	0	4.6544	–5.6001
H	0	5.6899	–5.9303
C	0	4.3686	–4.2251
H	0	5.1871	–3.5123